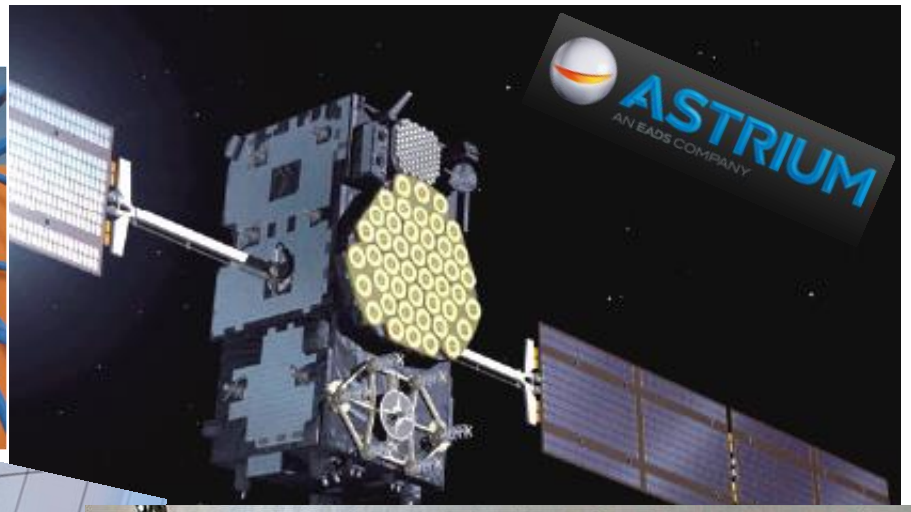

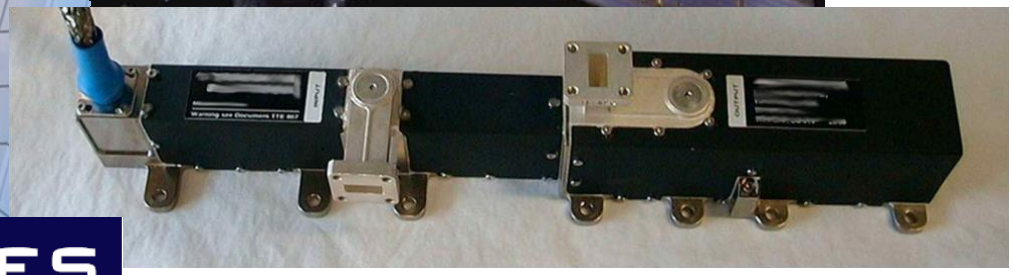

Chapter 3.2

TRAVELING WAVE TUBES (TWT)

History of Traveling Wave Tube (TWT)

1940 N.E. Lindenblad (Patent in USA)
1942/43 R. Kompfner (Univ. of Birmingham)
1945 J.R. Pierce, L.M. Field
(Bell Telephone Lab.)

Basic Idea : No frequency limiting cavities
but travelling wave structures

Slow wave with $v_{ph} \lesssim v_e < c$

1kV = 20 000 km/s = $\frac{1}{15}$ c_0

Helix with pitch s and
circumference $2\pi R$

$$v_{ph} = c_0 \frac{s}{2\pi R} = c_0 \sin\psi$$

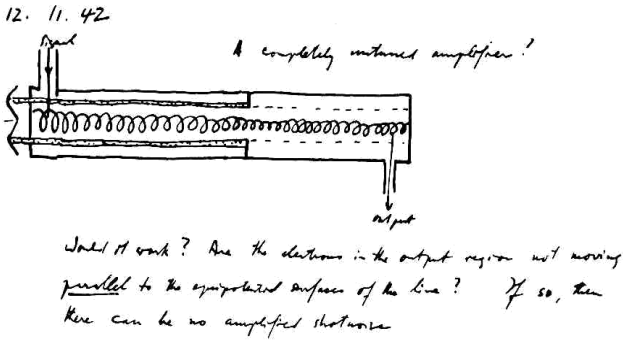

Long lasting and intensive interaction of electron beam with slow wave

PPM (Periodic-Permanent-Magnet) – Focussing

(a) Input Section : Velocity Modulation

(b) Attenuator : Attenuation
(Sever Loads) of Backward Waves
Electron Bunching

(c) Output Section: Induction of
amplified
RF - Currents.

(d) Depressed Collector: Energy Recovery

http://de.scribd.com/doc/60932762/9/TWT-Physics

Pioneers of TWT Development (1960)

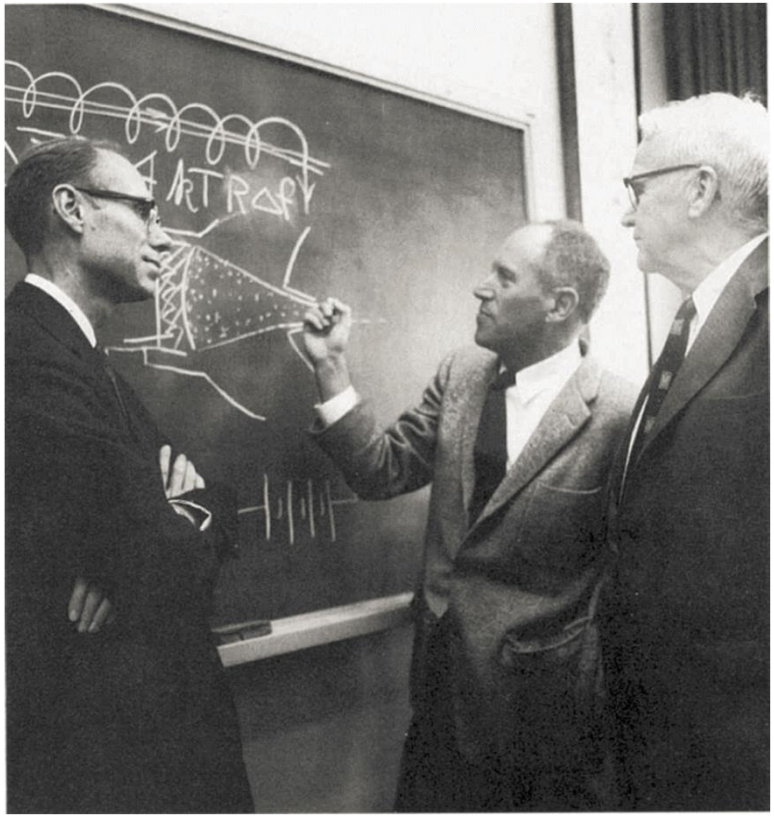

John Pierce, Rudolf Kompfner, Henry Nyquist

John Pierce

Applications (Example: Thales Electron Devices)

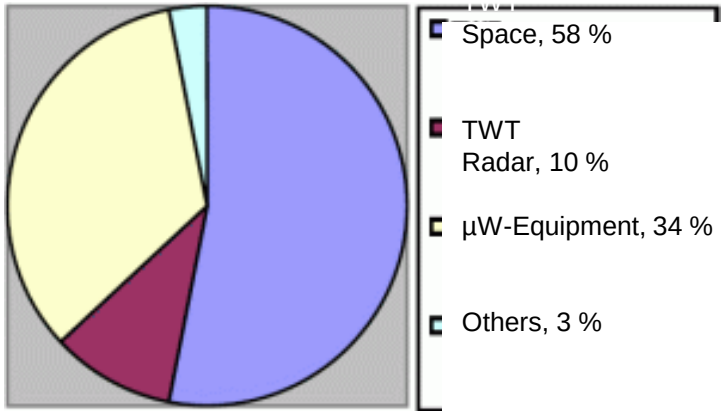

Example: THALES Electron Devices GmbH in Ulm

Turnover (2006): **99.6** Mio. Euro

TEDG develops Traveling Wave Tubes, mainly for Space Applications (Satellite TV Communication multimedia applications), but also for Radar.

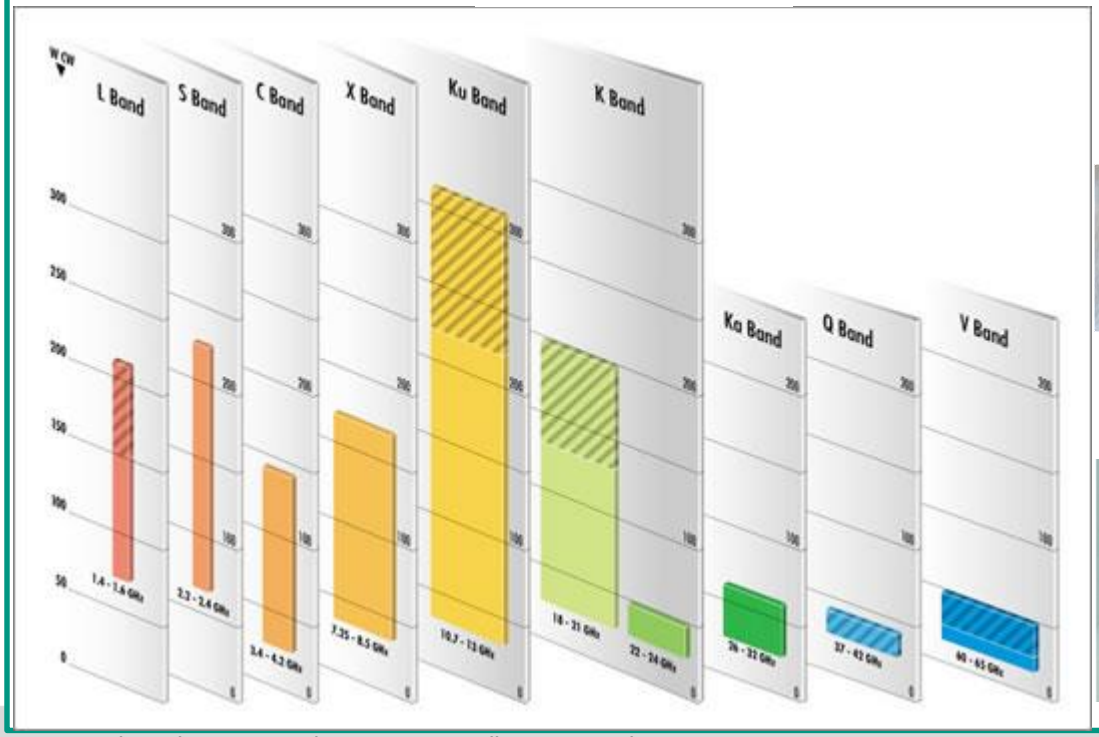

Ku-Band (TV-Satellites)

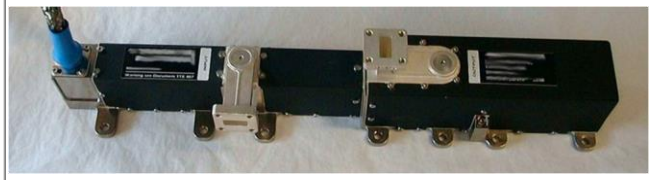

L-Band (Galileo)

Principle Setup of TWT

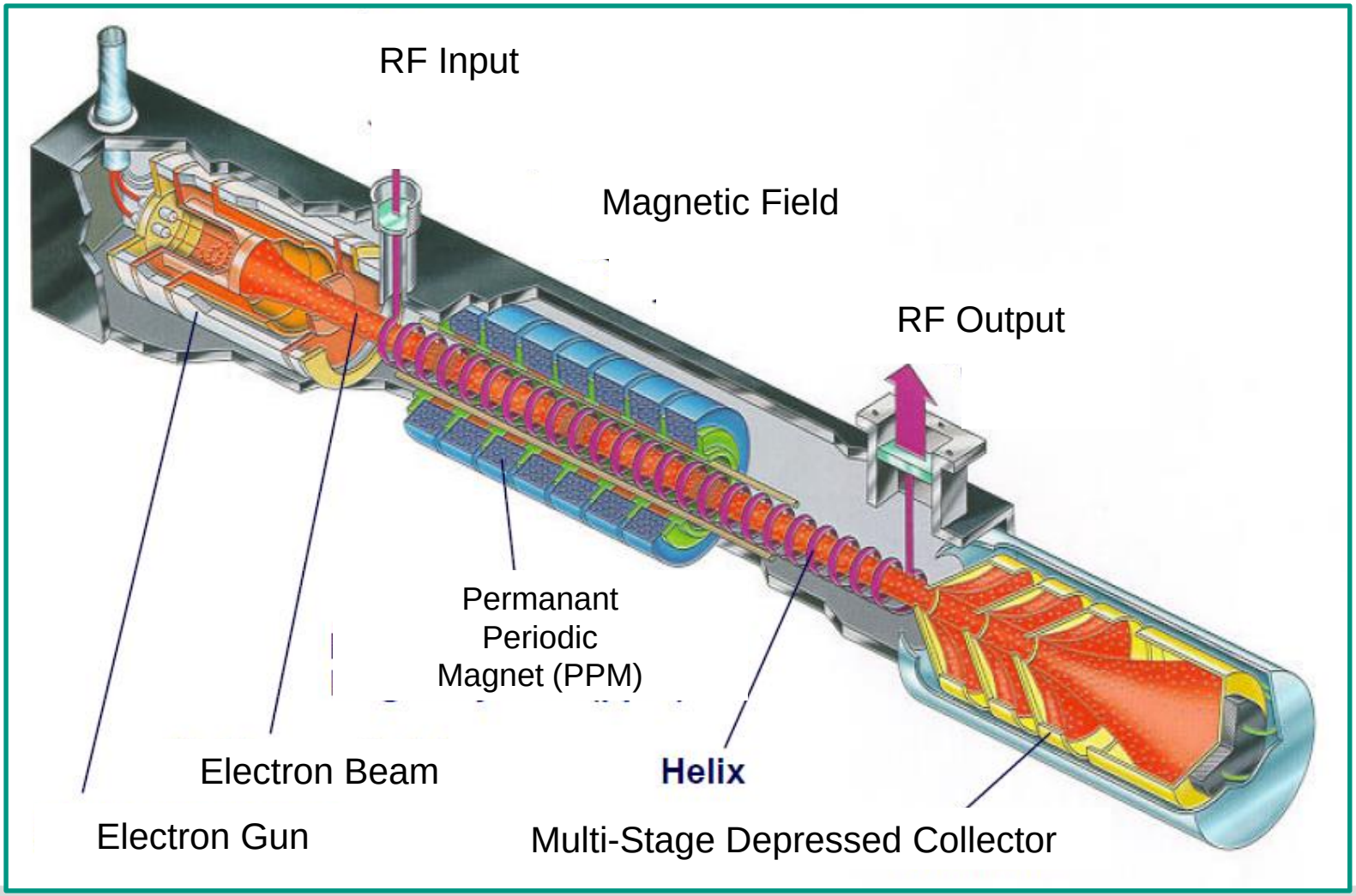

Schematic and Voltages of TWT

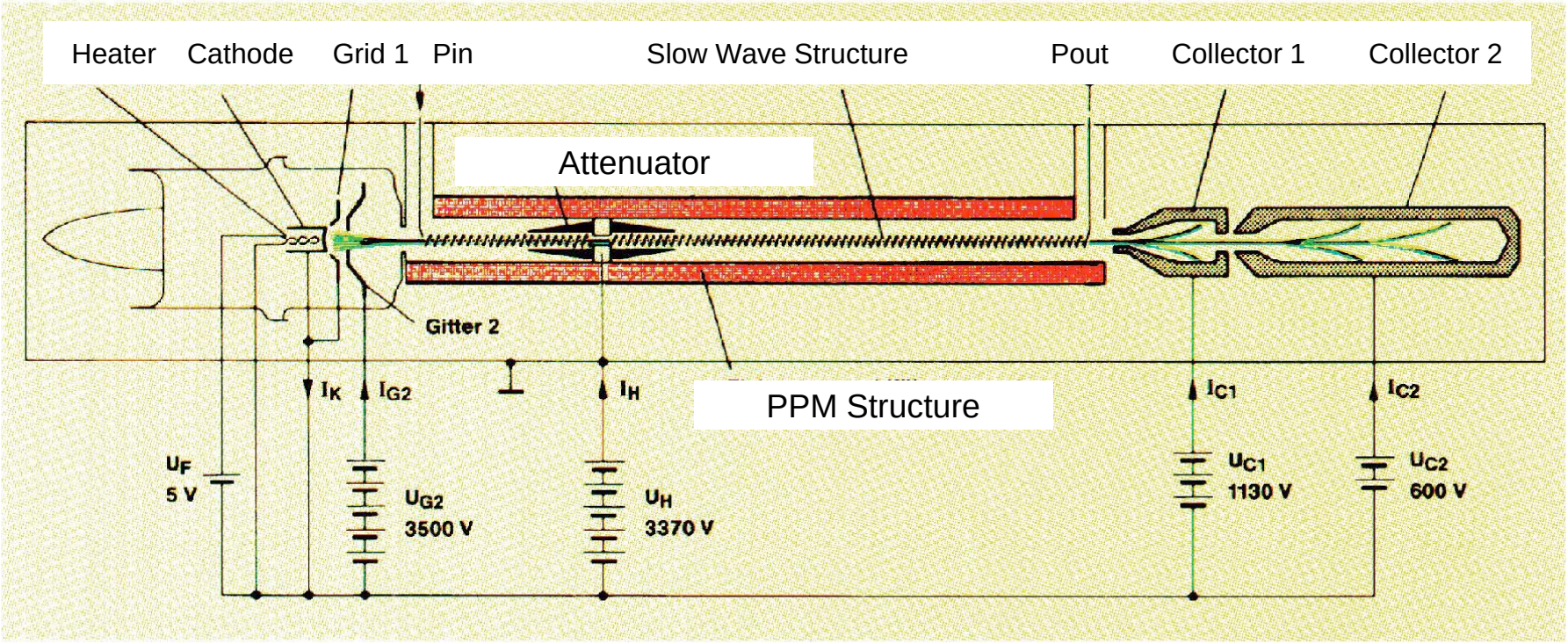

Elements of TWT:
Ku-Band TWT with and without Housing

Conduction Cooling

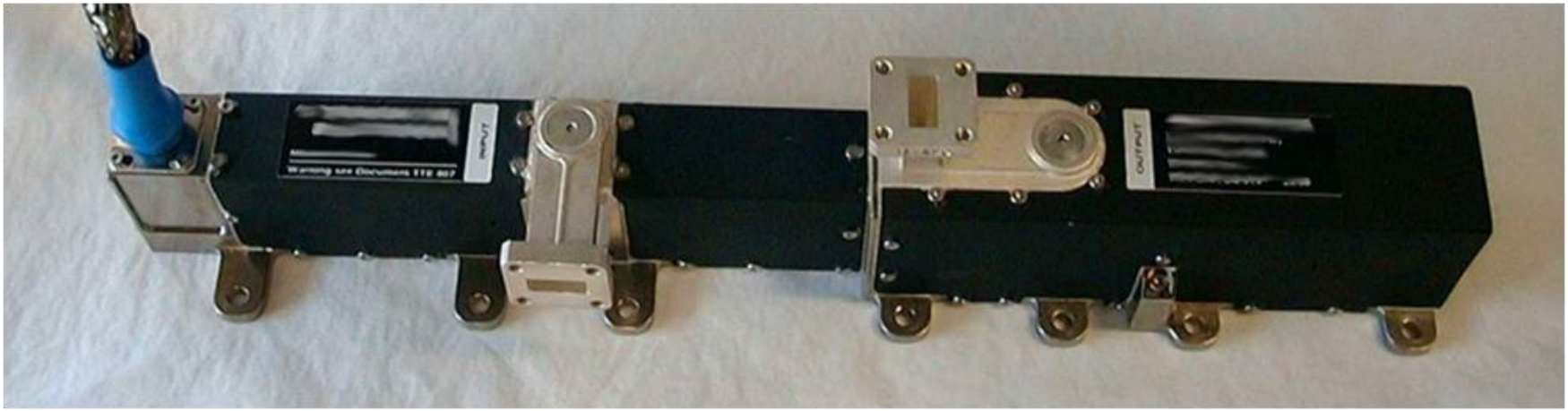

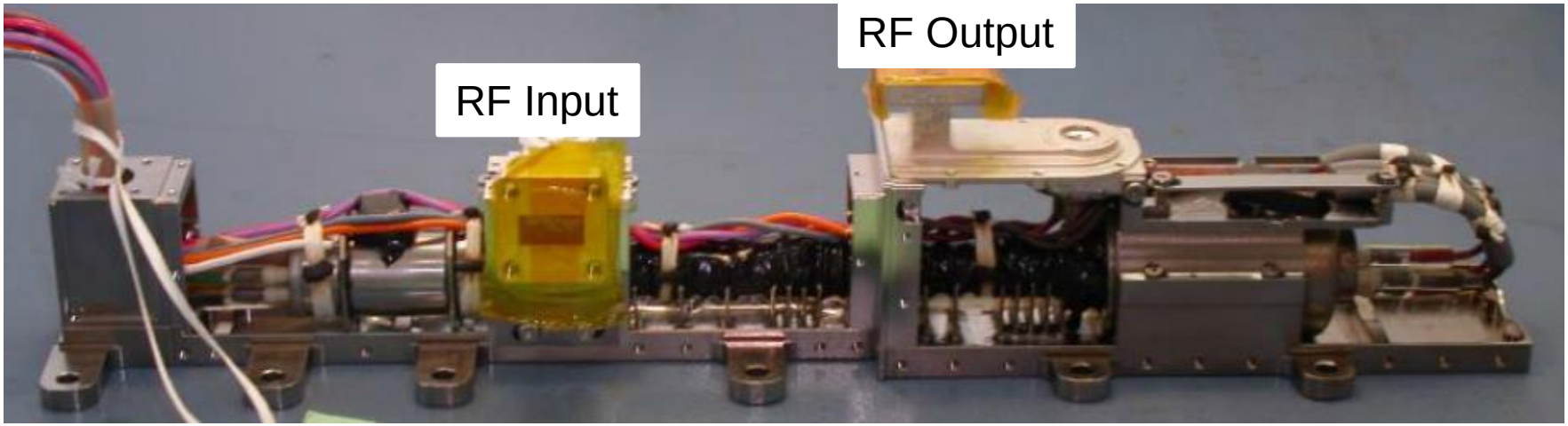

Principle of Slow-Wave Structures (Delay Lines)

- The delay line (e.g. helix) adjusts the RF wave phase velocity to the electron velocity.
- The input RF signal results in a density modulation within the electron beam.
- An attenuator along the delay line isolates the RF input from the RF output.
- The pitch angle of a helix delay line is optimized along the axis in order to improve RF-interaction and efficiency (decreasing pitch angle).

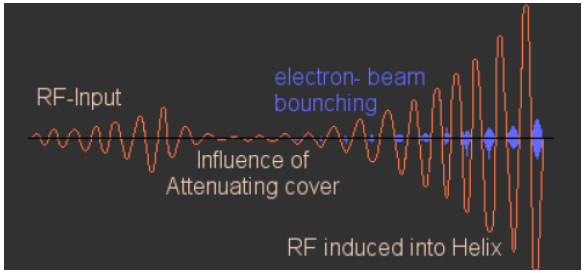

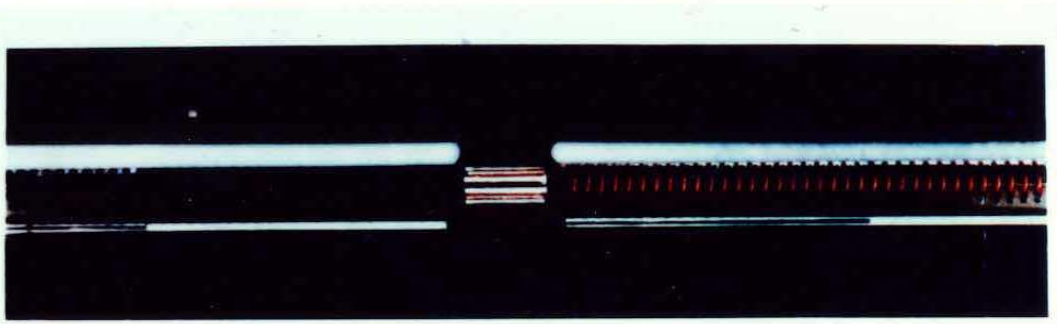

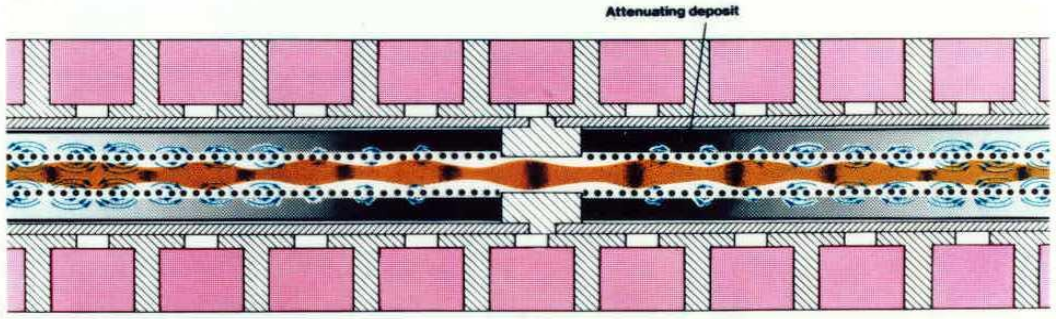

Various Delay Lines (Slow-Wave Structures)

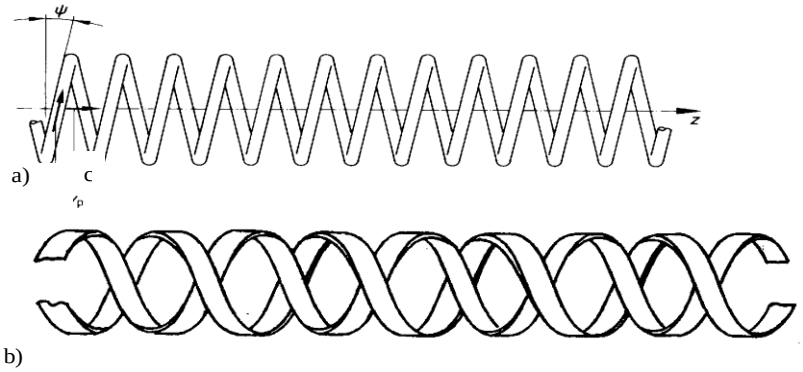

a) Helix delay line. The pitch angle ψ defines the RF phase velocity v_p. $v_p = c \cdot sin\psi = c \cdot s/2\pi R$; c = speed of light, s = axial pitch. b) Double tape helix.

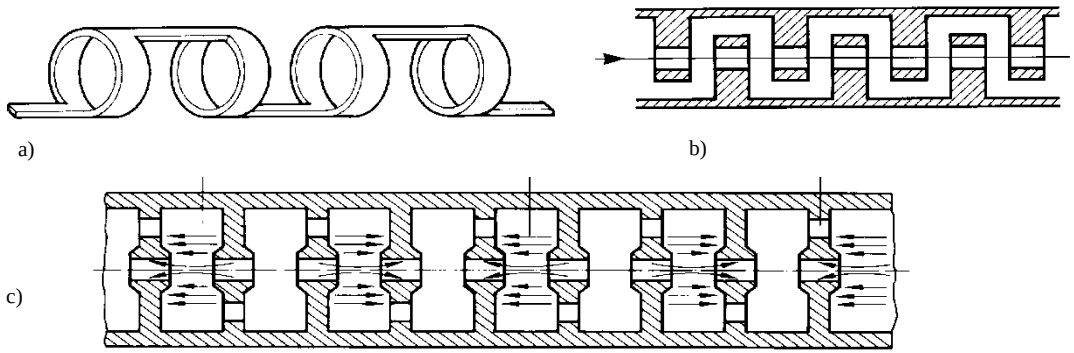

a) Ring-bar line, b) Interdigital- or comb- or folded-waveguide line, c) Coupled cavity line.

Slow - Wave Structures

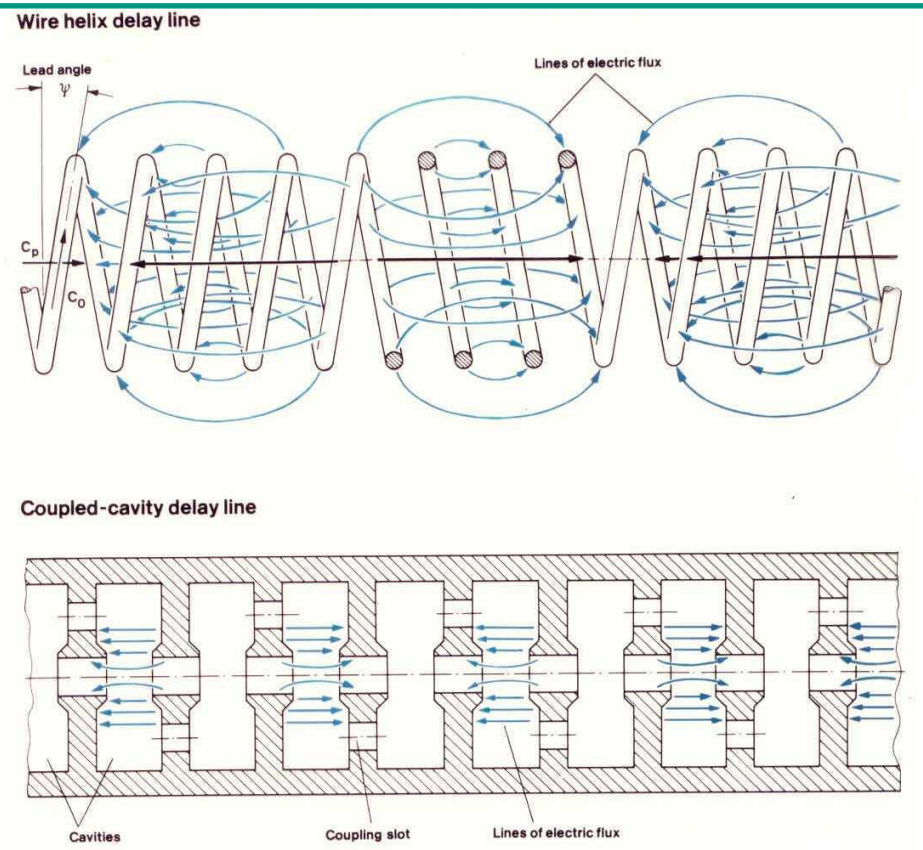

- Wire Helix
- Tape Helix
- Coupled Cavities (BW = 10%)

} Larger Bandwidth (BW = Octave)

} Higher Output Power

(a) Brazed Helix TWT (Thales Electron Devices)
3.0kW, 6GHz, BW = 10%, Gain = 57dB

(b) Coupled Cavity TWT (Hughes)
2.8kW, 8GHz, BW = 7%, Gain = 55dB

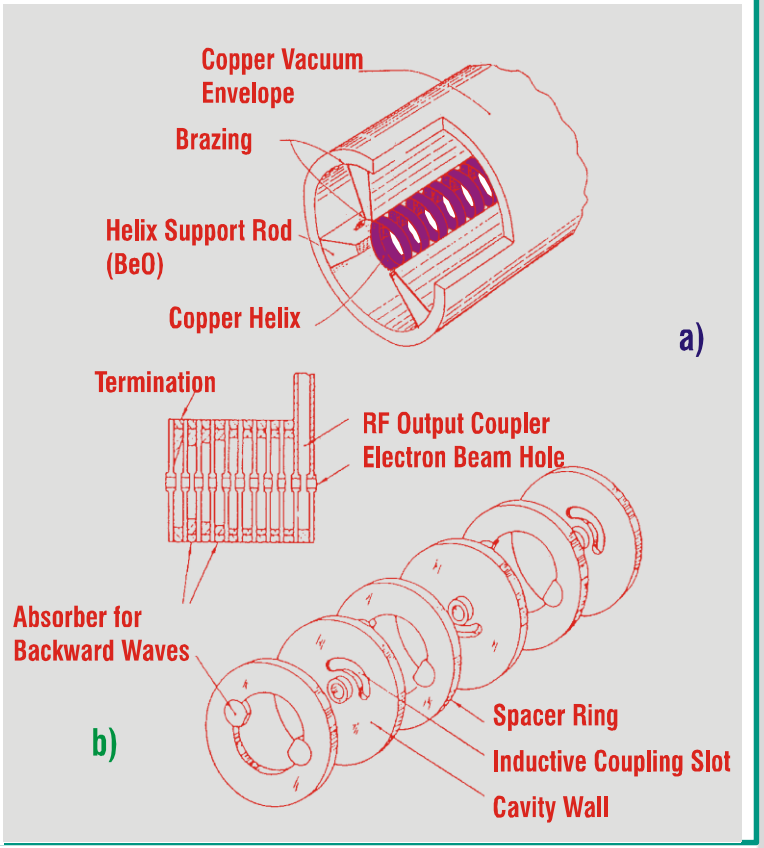

Helix Slow-Wave Structure

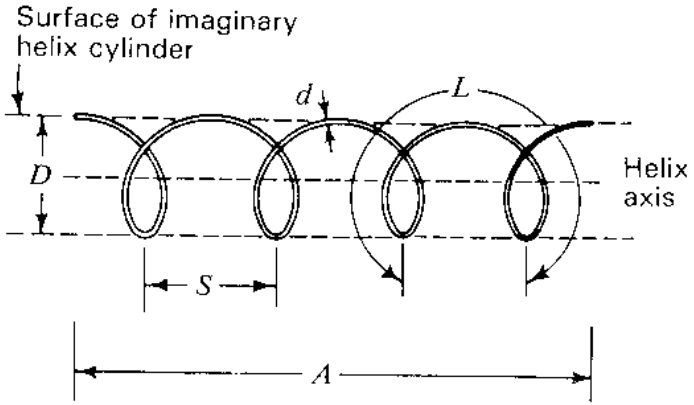

Basic helix geometry defining diameter (D), turn-to-turn pitch (S), axial length (A), circumference (C), turn length (L), and pitch angle (α).

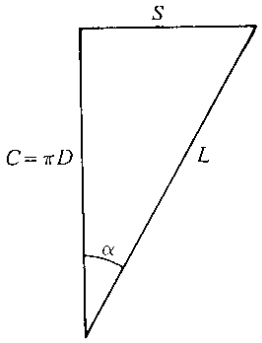

The relations between S, C, D, L and α are shown for a single turn that has been stretched out flat.

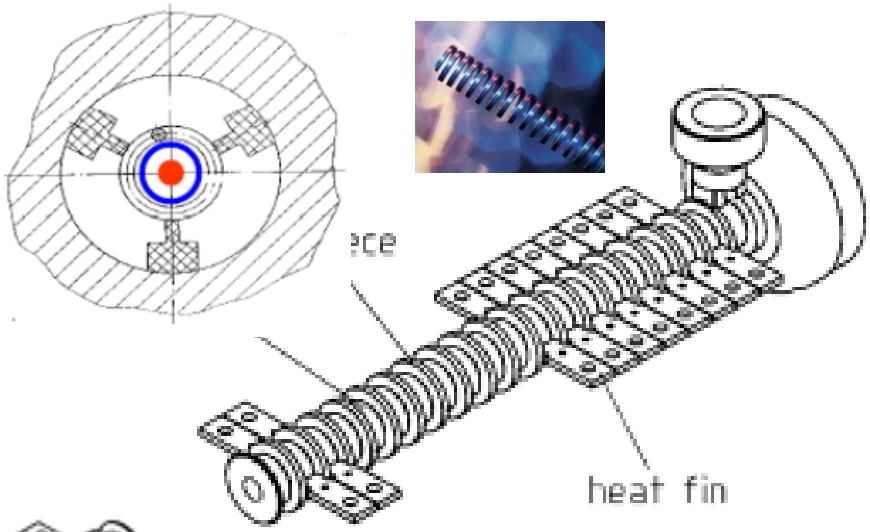

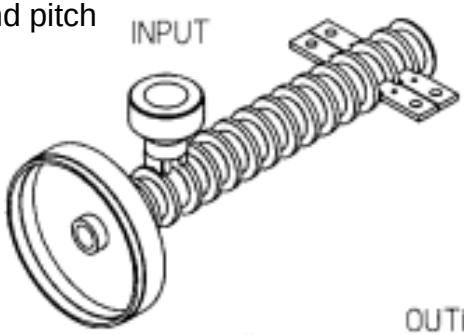

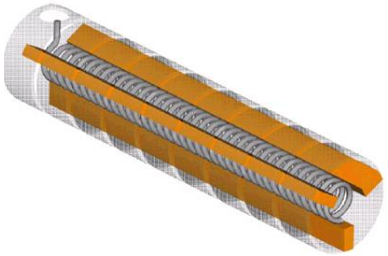

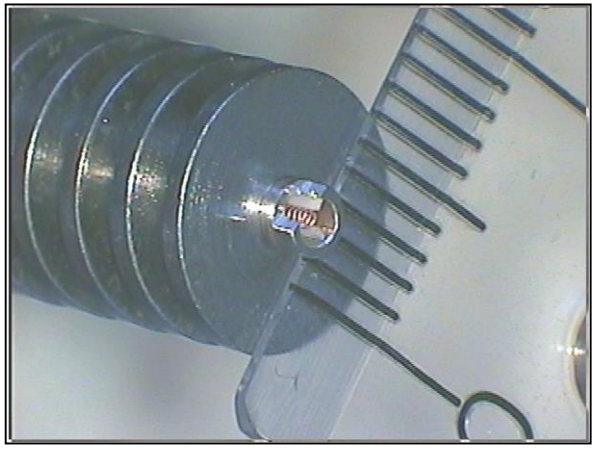

“Double-Comb Delay Line”

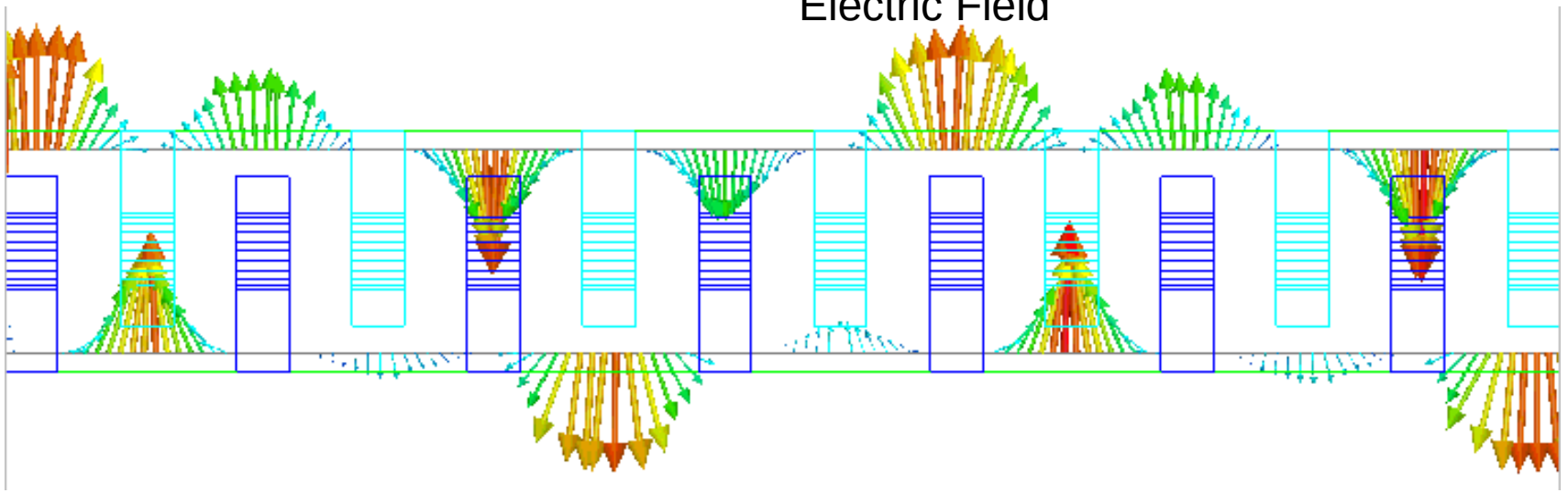

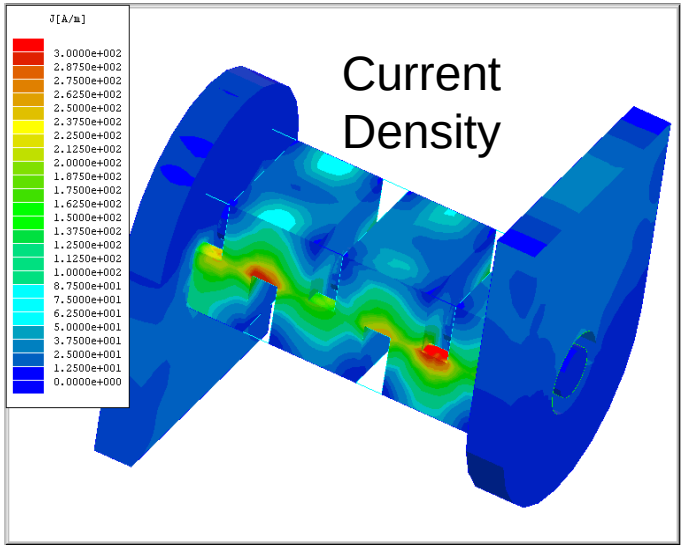

Application: Higher Power

Folded Waveguide Structure

Duality with Accelerator Structures – „Iris Loaded Waveguide“ Structures for CERN

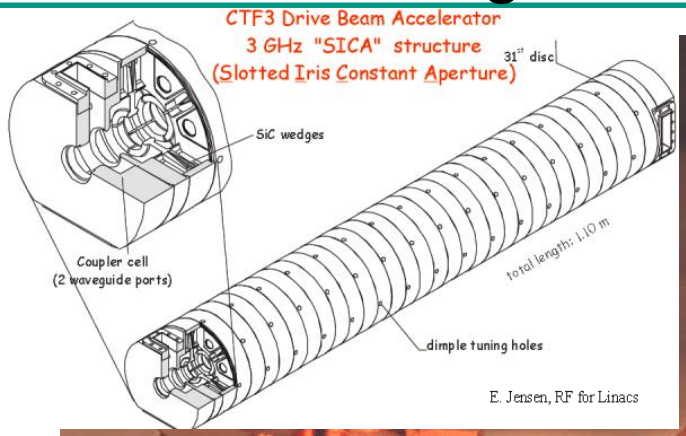

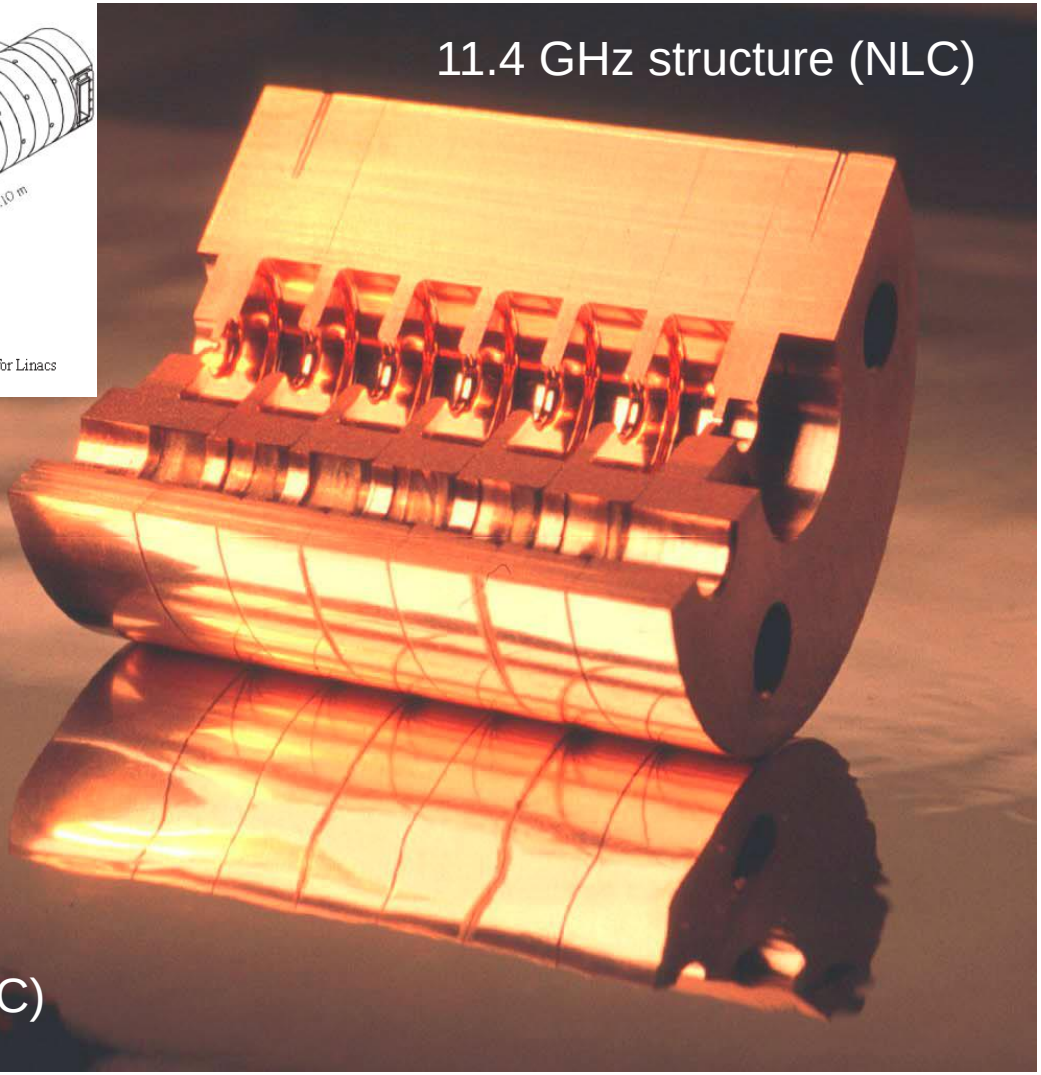

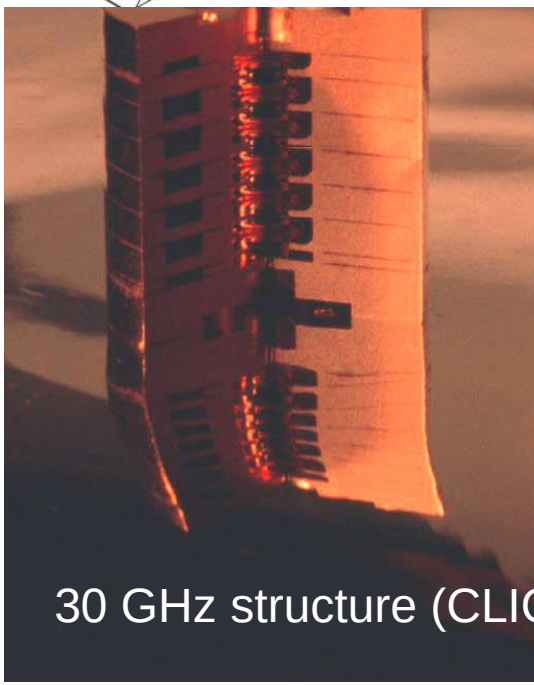

Optimization of Slow Wave Structures: The Brillouin-Diagram

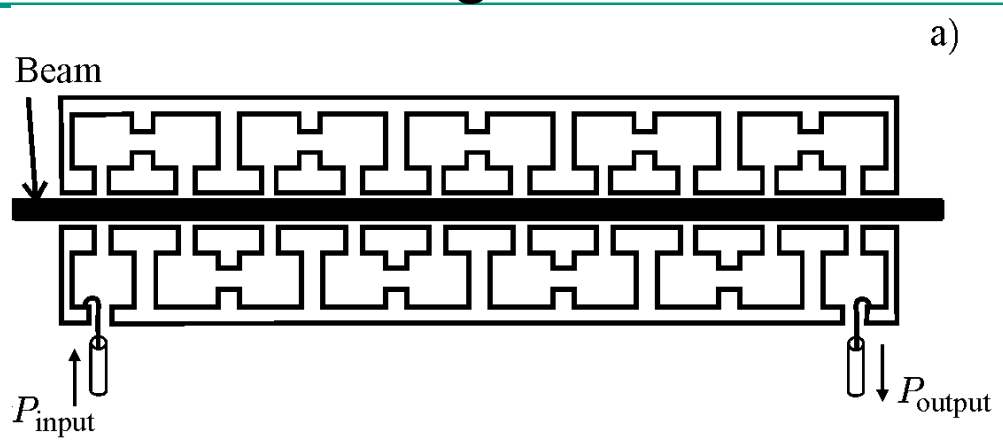

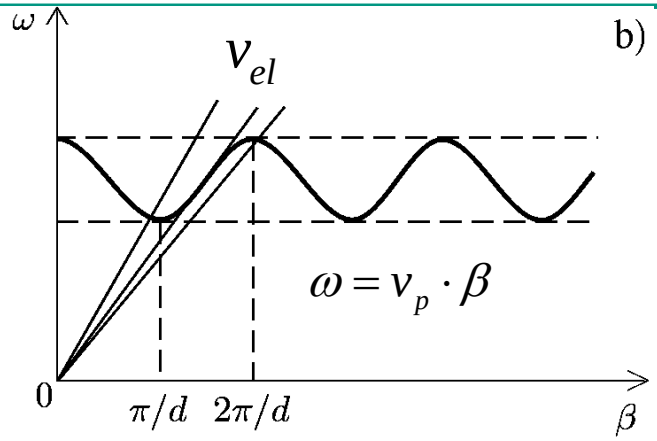

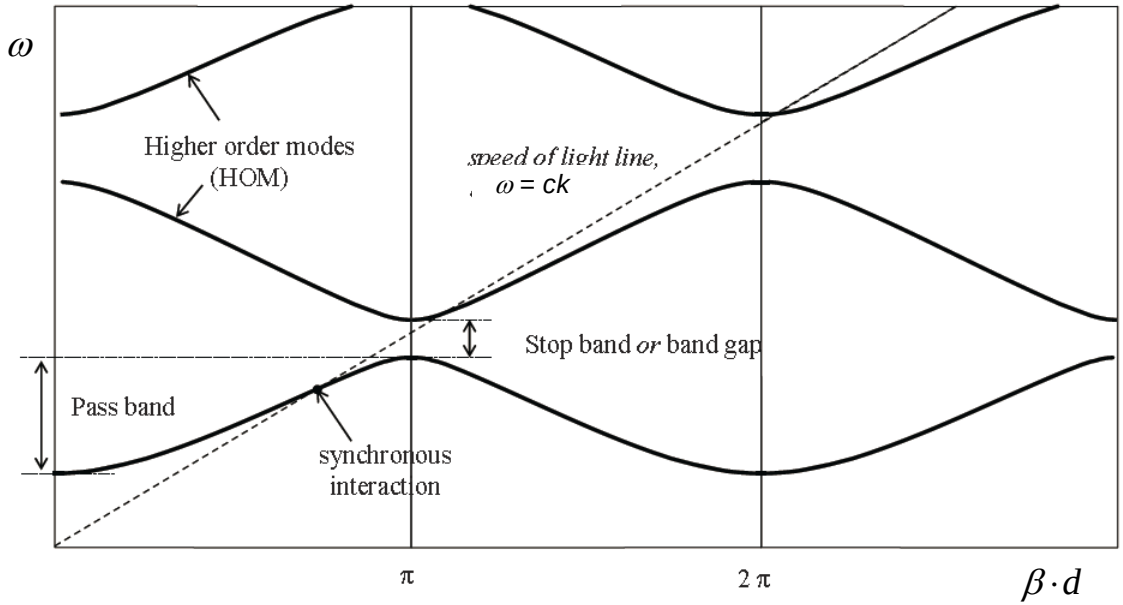

See Section 1.4

Definition: Phase- and group velocities

$v_p := \frac{\omega}{\beta} = \frac{k \cdot c}{\beta}$: phase velocity

$v_g := \frac{d\omega}{d\beta} = c\frac{dk}{d\beta}$: group velocity

$k := \frac{\omega}{c} = \frac{2\pi}{\lambda}$: wave constant

β : phase constant of propagating mode

Example:
E-Field Distribution at Different Points in the Dispersion Diagram of a Slow-Wave Structure

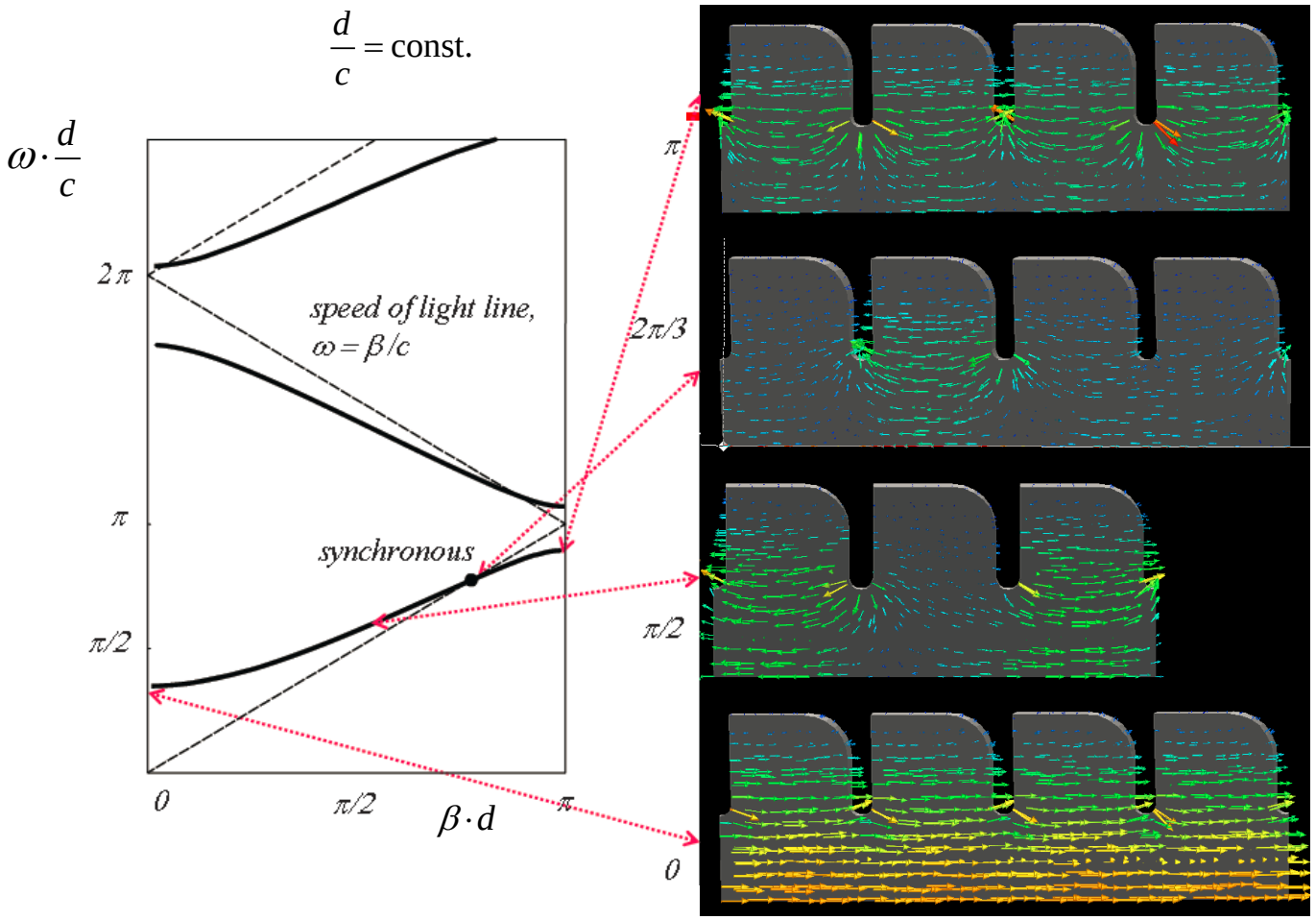

Source: E. Jensen, „RF for Linacs“

Equivalent Circuit of Slow-Wave Structure

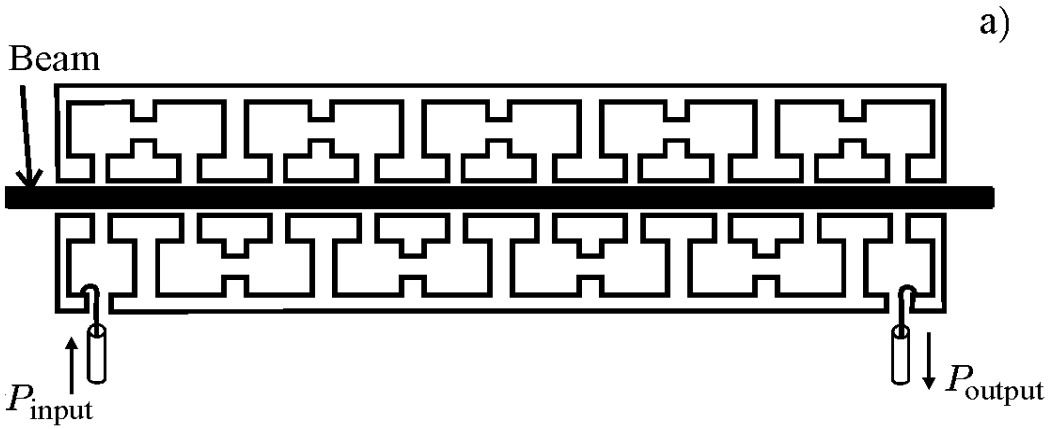

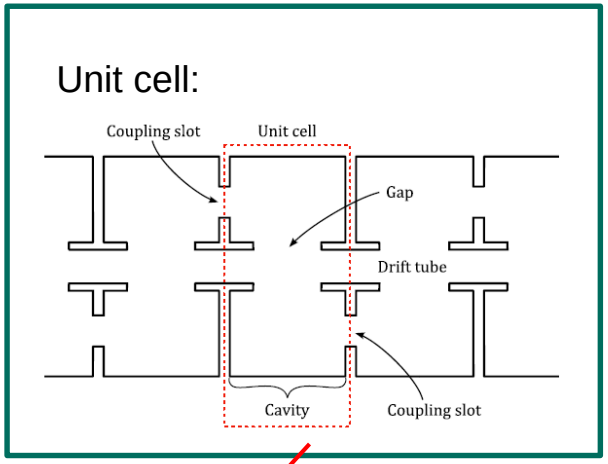

Chain matrix:

$$\begin{pmatrix} V_{rn} \\ -I_{rn} \end{pmatrix} = [T] \cdot \begin{pmatrix} V_{ln} \\ I_{ln} \end{pmatrix} .$$

For periodic boundary condition:

$$\begin{pmatrix} V_{rn} \\ -I_{rn} \end{pmatrix} = e^{-j\varphi} \cdot \begin{pmatrix} V_{ln} \\ I_{ln} \end{pmatrix}$$

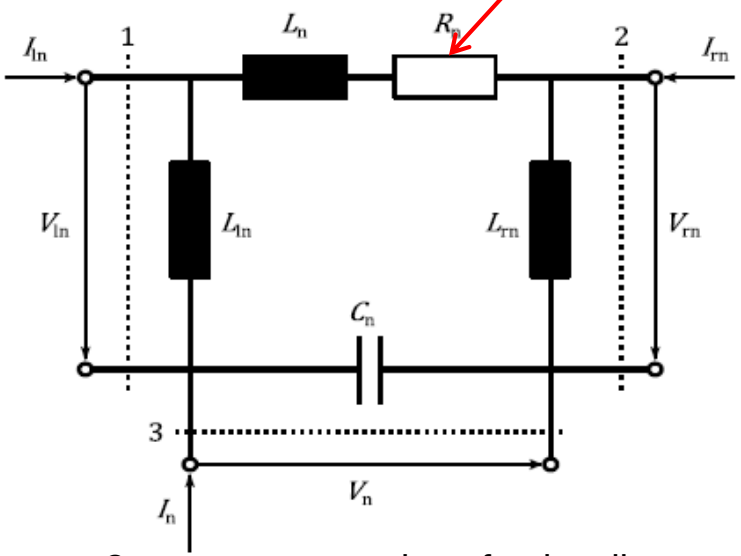

3-port representation of unit cell

Pierce Theory

The amplification process in a TWT is a complex mechanism as it involves two systems that are coupled: the EM wave on the delay line and the particles of the electron beam. The theory of EM waves as well as particle physics are needed to describe TWT operation.

The following section is subdivided into three parts. The first is concerned with modeling the EM waves along the delay line, while the second describes the electron beam. The third then takes into account the interaction of those two systems for synchronous operation. The presented derivation is also known as the Pierce theory and gives much insight into the physics of TWTs. It is named after John R. Pierce who first described the interaction in a TWT in a closed form [15]. The following derivations are adapted from [11] and are given here for the sake of completeness, since the conclusions drawn from this theory become important for subsequent chapters.

In the following all field quantities implicitly depend on time t and axial distance z as $\exp(j(\omega t - \beta z))$ with angular frequency ω and propagation constant β. Therefore, it follows that

$$\frac{\partial}{\partial t} = j\omega, \text{ and} \tag{2.2}$$

$$\frac{\partial}{\partial z} = -j\beta. \tag{2.3}$$

Source:
Principle of Traveling Wave Tubes, ser. The Artech House Radar Library. Artech House, Incorporated, 1994.
J. R, Pierce, Traveling-Wave Tubes, ser. Bell Telephone Laboratories. Van Nostrand, 1950.

Pierce Theory

The delay line can be described by means of a transmission line (TL). An incremental element of length Δz has an inductance L_ℓ and capacitance C_ℓ per unit length. An adequate equivalent circuit (EC) is shown in Figure 2.6. An additional RF current ΔI_1 is induced at point B due to the presence of the electron beam. Applying Kirchhoff's current law in this point and Kirchhoff's voltage law around the closed loop ABCD with $\Delta z \to 0$, respectively, the differential equations

$$\frac{\mathrm{d}V_C}{\mathrm{d}z} = -j\omega L_\ell \cdot I_L, \text{ and} \tag{2.4}$$

$$\frac{\mathrm{d}I_L}{\mathrm{d}z} = \frac{\mathrm{d}I_1}{\mathrm{d}z} - j\omega C_\ell \cdot V_C \tag{2.5}$$

are obtained. Using Equation (2.3) and substituting I_L from Equation (2.5) into Equation (2.4) leads to

$$V_C = \frac{\omega\beta L_\ell}{\beta^2 - \omega^2 L_\ell C_\ell} I_1. \tag{2.6}$$

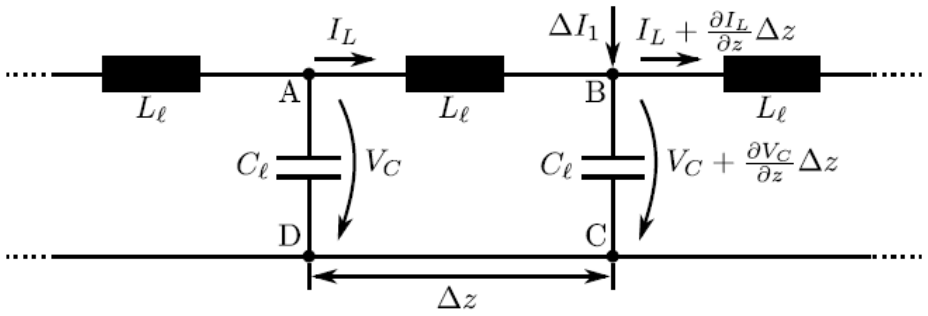

Pierce Theory

Assuming further that the electron beam travels close to the TL, the axial electric field E_z acting on the electrons can be calculated as

$$E_z = -\frac{\partial V_C}{\partial z} = j\beta V_C = \frac{j\omega\beta^2 L_\ell}{\beta^2 - \omega^2 L_\ell C_\ell} I_1. \tag{2.7}$$

Introducing the cold propagation constant β_c and circuit impedance Z_c

$$\beta_c = \frac{\omega}{v_p} = \omega\sqrt{L_\ell C_\ell} \quad \text{and} \quad Z_c = \sqrt{\frac{L_\ell}{C_\ell}}, \tag{2.8}$$

respectively, the electric field acting on the electron beam becomes

$$E_z = j\frac{\beta^2\beta_c Z_c}{\beta^2 - \beta_c^2} I_1. \tag{2.9}$$

Pierce Theory/ Space Charge Wave

In order to determine the propagation characteristics of EM waves along an electron beam, at first an infinite beam in transverse direction is considered. The propagation then follows from the solution of the wave equation with a source term stemming from the flow of negative charges. Since the transverse dimensions of the electron beam are assumed to be infinite, the following one-dimensional (1D) wave equation for the axial electric field E_z is obtained [11]

$$\frac{\partial^2}{\partial z^2}E_z + k^2 E_z = -j\omega\mu_0 J_1 - \frac{1}{\epsilon_0}\frac{\partial}{\partial z}\rho_1, \tag{2.10}$$

where $k = \omega/c$ is the free-space wavenumber with c denoting the speed of light, ρ is the space-charge density, J is the current density, and μ_0 and ϵ_0 are the vacuum permeability and permittivity, respectively. The subscripts 0 and 1 denote DC and RF quantities, respectively. Applying Equation (2.3) to Equation (2.10) leads to

$$(\beta^2 - k^2)E_z = j\omega\mu_0 J_1 - \frac{j\beta}{\epsilon_0}\rho_1. \tag{2.11}$$

The current density J is the product of the space-charge density ρ and the electron velocity u, i.e., $J = \rho u$. Both ρ and u are assumed to have a DC and an RF component, therefore

$$\rho = \rho_0 + \rho_1 \cdot e^{j\omega t} \text{ and} \tag{2.12}$$

$$u = u_0 + u_1 \cdot e^{j\omega t}. \tag{2.13}$$

Pierce Theory/ Space Charge Wave

A standard small-signal assumption can be applied, if RF quantities are much smaller than their DC counterparts. The product of two RF quantities can be neglected in this case and thus

$$J_1 \approx \rho_0 u_1 + \rho_1 u_0. \tag{2.14}$$

Using the continuity equation of the electron current density

$$\nabla \cdot \mathbf{J} + \frac{\partial \rho}{\partial t} = 0 \quad \text{or} \quad -j\beta J_1 = -j\omega\rho_1 \tag{2.15}$$

it follows from Equation (2.14) that

$$J_1 = \frac{\rho_0}{1 - \frac{\beta u_0}{\omega}} u_1. \tag{2.16}$$

The equation of motion for the electrons under the influence of an axial electric field E_z is given by

$$\frac{\mathrm{d}u}{\mathrm{d}t} = \frac{\partial}{\partial t} u_1 + u_0 \frac{\partial}{\partial z} u_1 = (j\omega - j\beta u_0) \cdot u_1 = -\eta_\mathrm{e} E_z, \tag{2.17}$$

Pierce Theory/ Space Charge Wave

where η_e is the electron charge-to-mass ratio. Combining Equations (2.16) and (2.17) leads to

$$J_1 = j\frac{\omega\rho_0\eta_e}{(\omega-\beta u_0)^2}E_z = j\omega\epsilon_0\frac{\omega_p^2}{(\omega-\beta u_0)^2}E_z, \tag{2.18}$$

where the plasma frequency $\omega_p^2 = (\eta_e\rho_0)/\epsilon_0$ has been introduced. It is convenient to replace ρ_0 and u_0^2 by J_0/u_0 and $2\eta_e V_0$, respectively. Additionally, the current densities can be replaced by the corresponding currents, since a one-dimensional problem is considered here, i.e.,

$$I_1 = \frac{j\beta_e I_0}{2V_0(\beta_e-\beta)^2}E_z, \tag{2.19}$$

where $\beta_e = \omega/u_0$ is the electronic propagation constant.

If the transverse dimensions of the electron beam are finite, the above derivation still holds. However, the plasma frequency ω_p has to be replaced by the reduced plasma frequency ω_q according to

$$\omega_q = F\cdot\omega_p, \tag{2.20}$$

where F is the plasma reduction factor. It depends on the shape and size of the electron beam and the metallic beam tunnel in which it travels [11].

Pierce Theory/ Interaction

Now that the EM waves on the delay line and the space-charge waves on the electron beam are described individually, they can be combined to describe interaction. Therefore, Equations (2.9) and (2.19) have to be fulfilled simultaneously. Interaction between the systems mainly depends on synchronism, i.e., only those parts of the EM wave interact with the beam that have approximately the same axial phase velocity as the velocity of the electrons. The synchronous operation is briefly discussed here, because it gives crucial insights into the topic and will be helpful for later discussions. For asynchronous operation and more involved considerations like the influence of loss and noise, the reader is kindly referred to [11].

To describe the beam-wave interaction Equations (2.9) and (2.19) are combined which results in the so-called determinantal equation

$$1 = \frac{\beta_\mathrm{e} I_0}{2V_0(\beta_\mathrm{e} - \beta)^2} \frac{\beta^2 \beta_\mathrm{c} Z_\mathrm{c}}{(\beta_\mathrm{c}^2 - \beta^2)}. \tag{2.21}$$

Pierce further introduces the gain parameter C by

$$C^3 = \frac{Z_\mathrm{c} I_0}{4V_0} \tag{2.22}$$

Pierce Theory/ Interaction

which is usually a very small quantity, with typical values between 10^{-2} and 10^{-1}.

Equation (2.21) is a fourth-order polynomial whose solutions yield the four propagation constants of the eigenmodes of the coupled system. Assuming forward-traveling modes, the coupled propagation constant β can be written under the assumption of synchronous waves, i.e., $\beta_e = \beta_c$, as

$$\beta = \beta_e + \xi, \tag{2.23}$$

where it is further supposed that β differs only by a small amount ξ from β_e. Introducing this into Equation (2.21) leads to

$$\frac{\beta_e^2(\beta_e^2 + 2\beta_e\xi + \xi^2)}{\xi^2(2\beta_e\xi + \xi^2)} 2C^3 + 1 = 0. \tag{2.24}$$

Since ξ is a very small quantity compared to β_e, ξ^2 can be neglected in comparison to $\beta_e\xi$ in the denominator. The same holds for $\beta_e\xi$ and ξ^2 compared to β_e^2 in the numerator. With these approximations Equation (2.24) can be directly solved for ξ to obtain

$$\xi = \sqrt[3]{-1}\beta_e C. \tag{2.25}$$

Pierce Theory/ Interaction

The three complex roots are then

$$\xi_1 = \left(\frac{1}{2} + j\frac{\sqrt{3}}{2}\right)\beta_e C, \tag{2.26}$$

$$\xi_2 = \left(\frac{1}{2} - j\frac{\sqrt{3}}{2}\right)\beta_e C, \text{ and} \tag{2.27}$$

$$\xi_3 = -\beta_e C, \tag{2.28}$$

and the respective propagation constants follow from Equation (2.23).

Remembering now that all waves are assumed to propagate as $\exp(j(\omega t - \beta z))$, it becomes apparent that

1. all three modes still travel in forward direction, since C is a small quantity,
2. two waves travel at the same speed, one growing and the other decreasing exponentially, and
3. one wave travels faster than the others and has a constant amplitude.

The fourth wave can be obtained by assuming a backward-traveling wave with a velocity close to that of the circuit in absence of the beam. The result is another fast wave with constant amplitude traveling in backward direction.

These considerations are important for Chapter 4 where coupled dispersion diagrams are calculated to determine the characteristic impedances of the coupled modes in order to minimize reflections at couplers and severs under hot operating conditions.

Small-Signal Theory of Pierce (III)

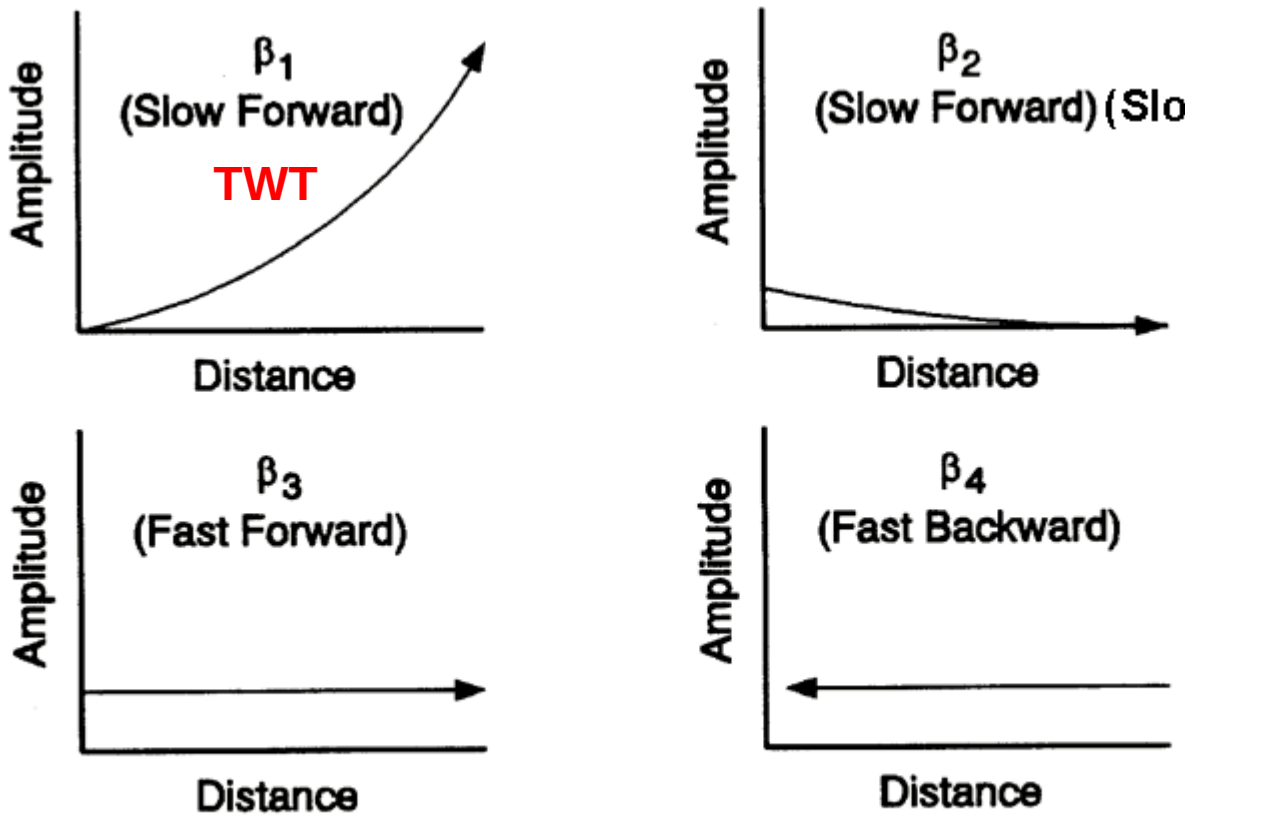

The four possible waves propagating along the delay line of a TWT.

Distribution of Electric Field And Space-Time Diagram

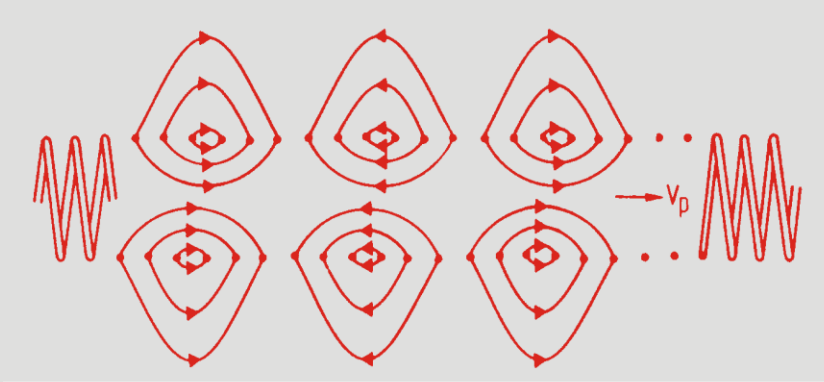

Electric field of travelling wave at a fixed time and axial component E_z and one wavelength

$\lambda_z = \lambda \sin \psi$ in axial direction

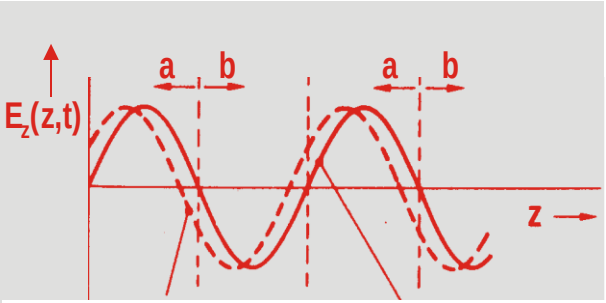

Electron Density Axial E-Field

Axial distribution of axial component E_z of travelling wave at fixed time and electron bunching in deceleration region.

a : Deceleration
b : Acceleration

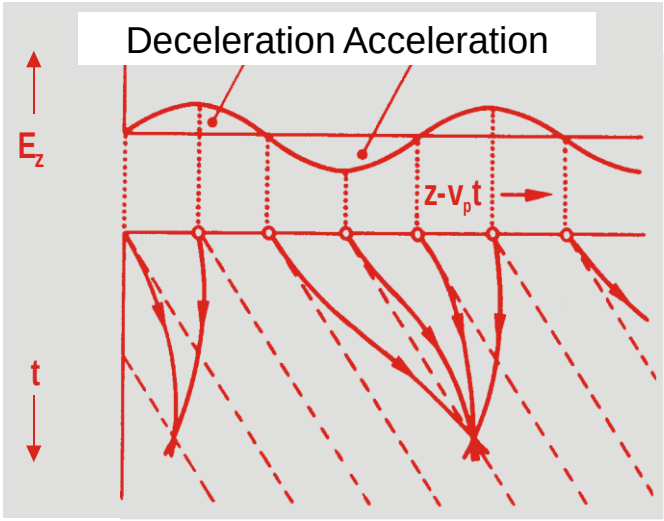

Longitudinal field E_z and distance - time curves of beam electrons with reduced $z-v_pt$ coordinate

(Trajectories are not straight lines as for klystrons due to changing electron velocity)

Bunching Process in TWT (Applegate-Diagram)

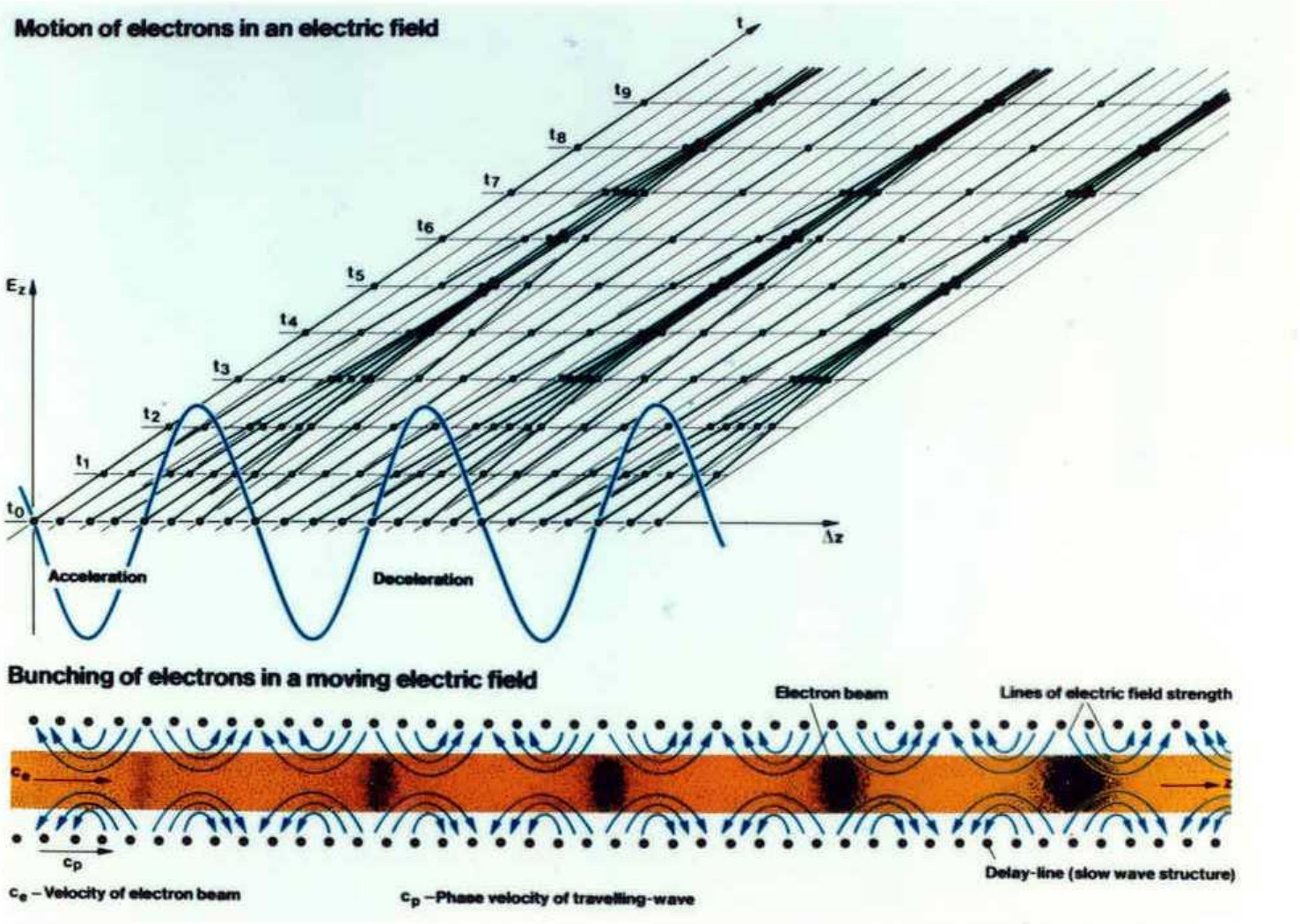

TWT Electron Gun (I)

Wehnelt cylinder is focusing electrode.

Cathode temperature 930°C to 1000°C

Modern cathodes are MM-type:
Tungsten-Osmium Matrix
(low work function and long-lifetime).

Ceramic stacks for insulation.

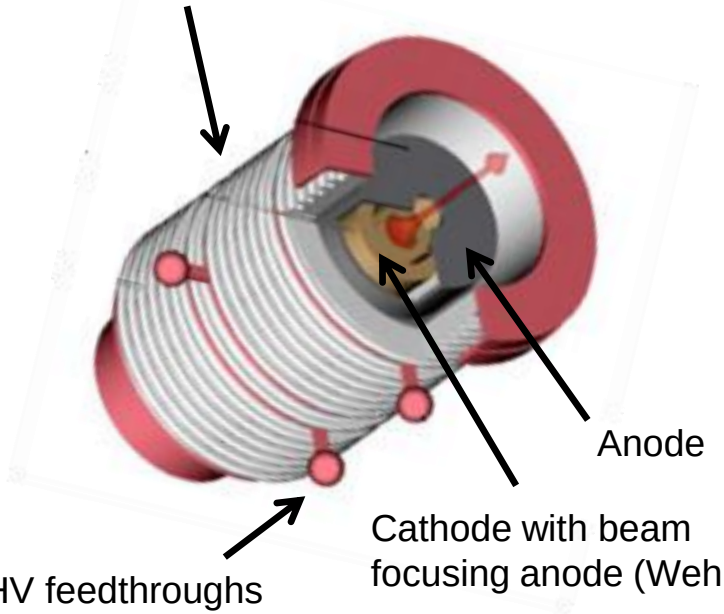

TWT Electron Gun (II)

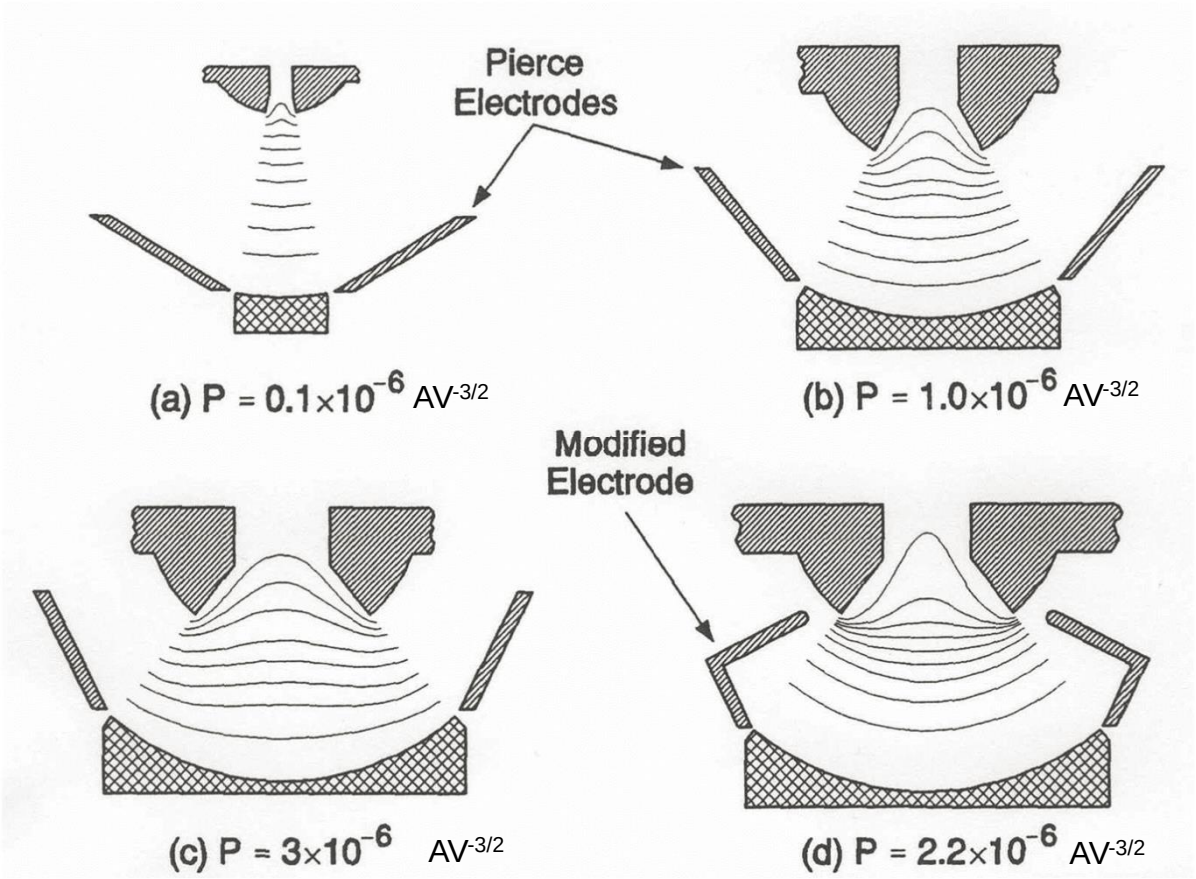

Perveance (***P***)

of space-charge limited diode

(„**Space charge constant**“)

$$I = \frac{4\pi}{9}\sqrt{2}\varepsilon_0\sqrt{\frac{q}{m}}\frac{r^2}{d^2}\cdot U^{\frac{3}{2}} = P\cdot U^{\frac{3}{2}}$$

$$P$$

(see Section 2.1)

Perveance depends on geometry only.

The Pierce electrode is kept on cathode potential in all cases. The perveance increases with smaller cathode to anode distance and larger half cone angle θ (larger width of cathode).

TWT Electron Gun (III)

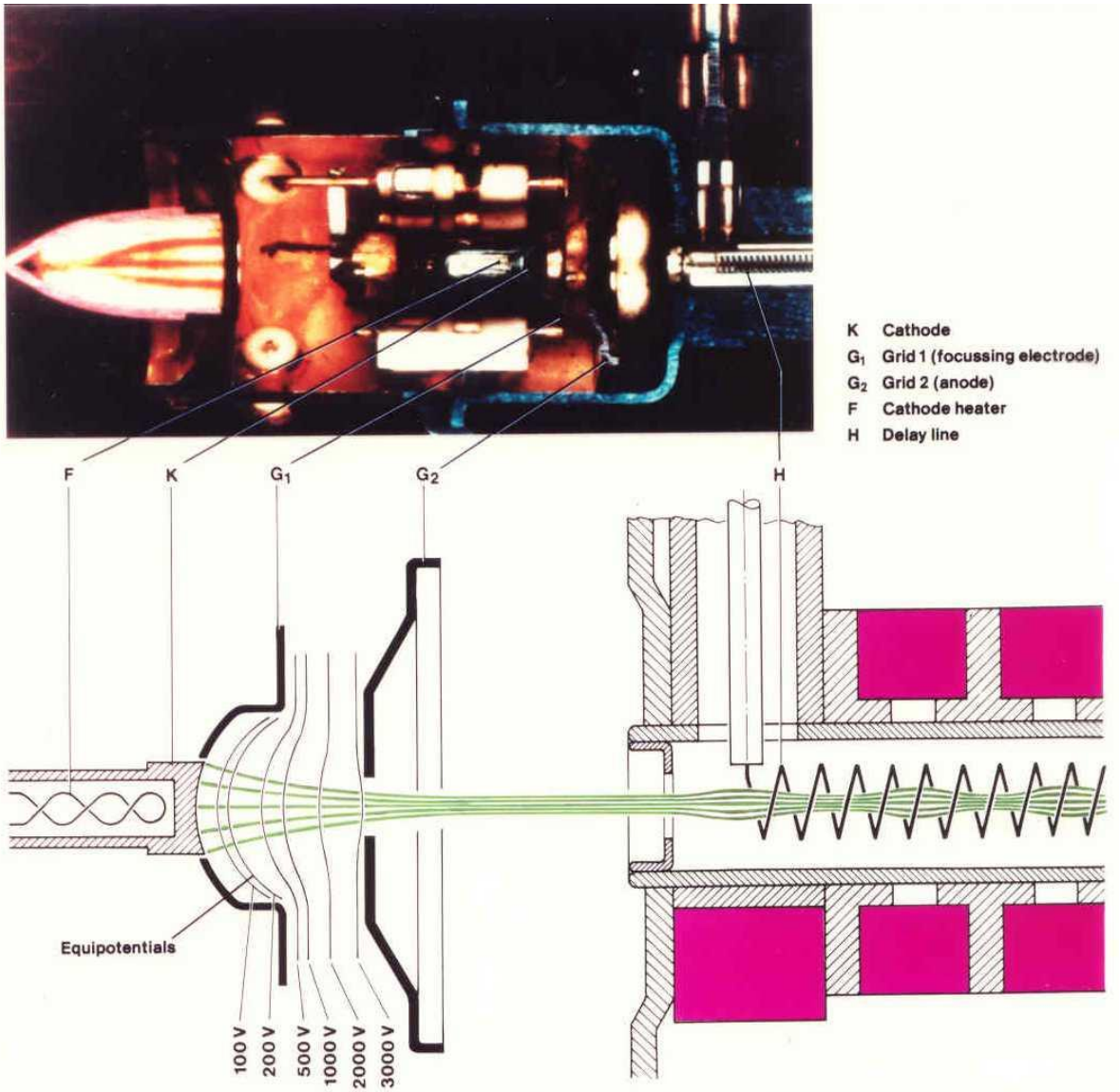

Focussing of Electron Beam into Slow Wave Structure

"Golden" trajectory and beam envelope from a 150 mA, 7.5kV modified Pierce gun into a 1mmϕ grounded tunnel, B_{peak} = 0.325 T

simulated with 2D-gun program and visualised with virtual reality shareware code by W. Schwertfeger TED, Ulm

The peak PPM magnetic field should be 1.2 to 2 times the socalled Brillouin field to guarantee a save focusing of an electron beam over the interaction length of a TWT.

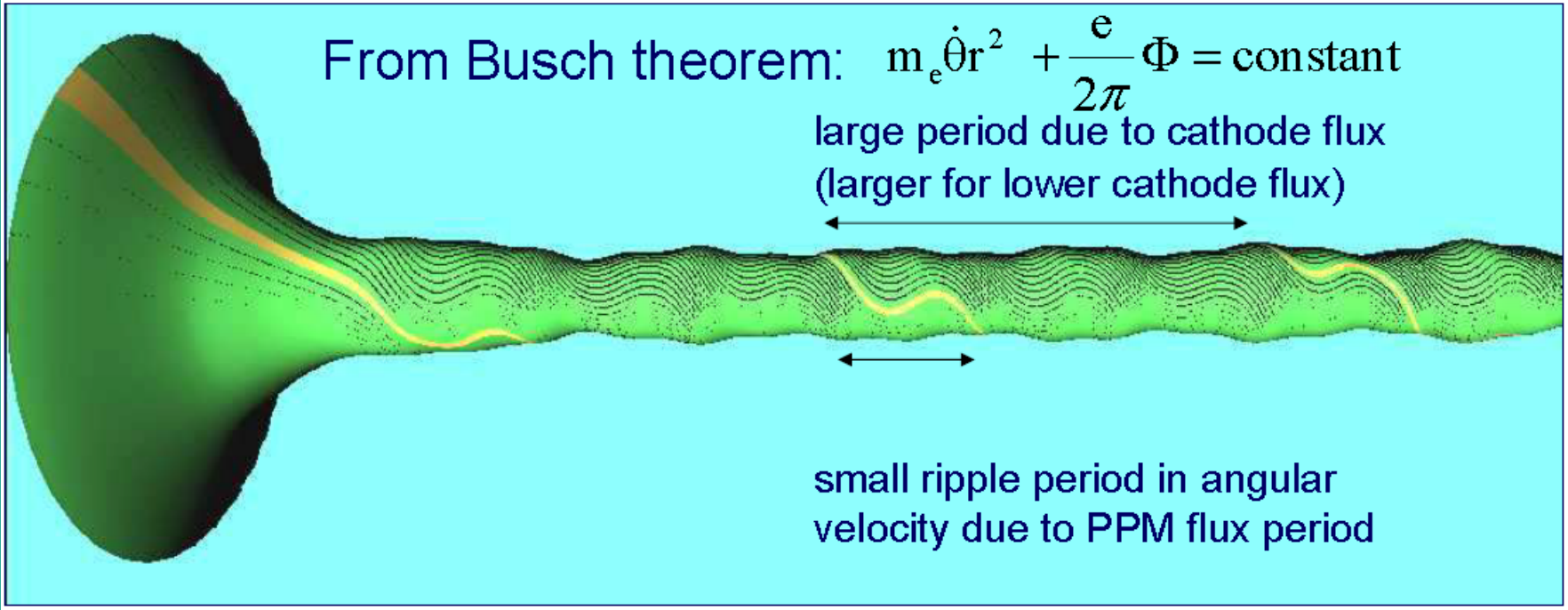

Different scaling in r and z direction! r = 10x

Beam Focusing over Delay Line Length

Repulsive Space Charge and Attractive Magnetic Forces in a Charged Particle Beam

For a uniform cylindrical charged particle beam with uniform axial velocity v, it can be shown that the radial F_{sc} forces at radius r on a charged particle are given by:

$$F_{sc} = Qe/(2\pi r\, \varepsilon_0)$$ outward radial space charge force

$$F_m = Qe\, \mu_0\, v^2/(2\pi r)$$ inward radial magnetic force

where Q is the total charge per unit length inside the radius r.

Inserting the physical identity $\varepsilon_0\, \mu_0 = 1 / c^2$ into the ratio of both self forces one simply obtains:

$$F_{sc} / F_m = c^2 / v^2$$

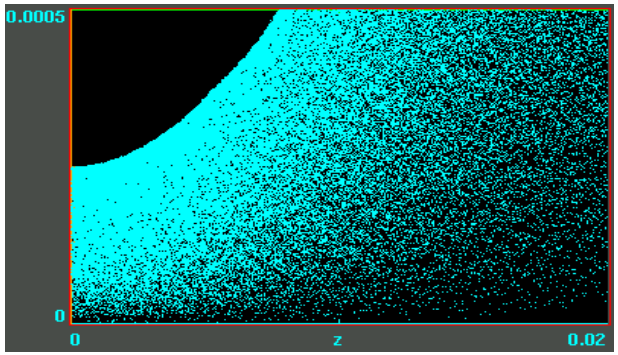

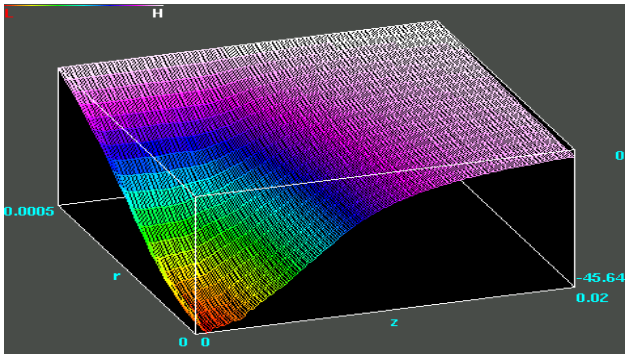

Electron distribution and space charge potential using XOOPIC, a 2.5 dimensional particle in cell (PIC) code developed by the Berkeley University in California. Simulation parameters: I_{beam} = 110 mA, V_{beam} = 7.5 kV, r_{beam} = 0.25 mm radius of beam and r_{tube} = 0.5 mm radius grounded tubing.

Magnetic Focusing

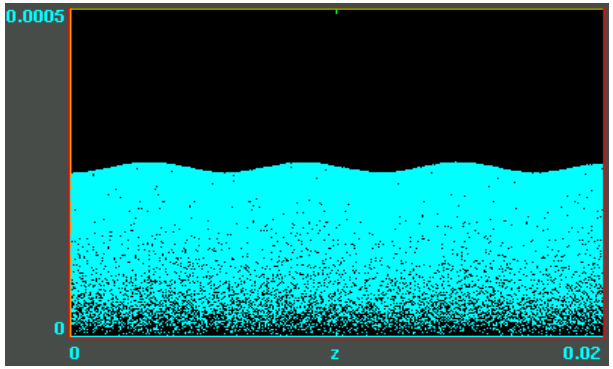

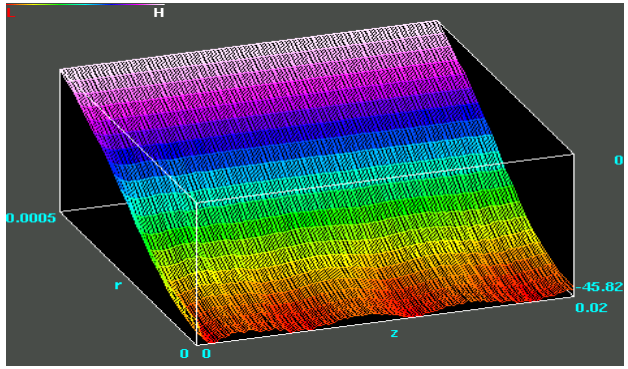

Particle in cell simulation of a 110 mA, 7.5 kV, 0.25 mm radius electron beam in a 0.5 mm radius grounded metal tubing as simulated with XOOPIC, in a homogeneous magnetic field with B_z = 0.33 T.

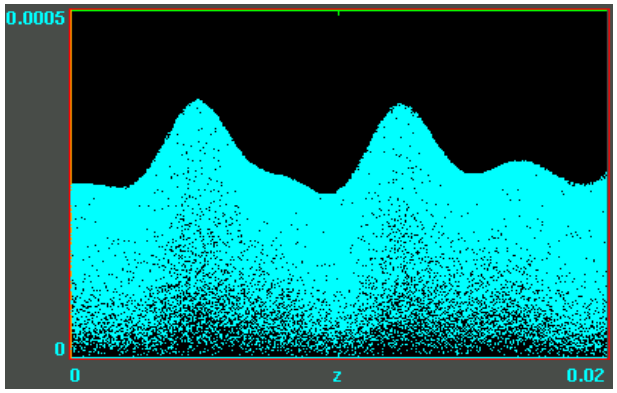

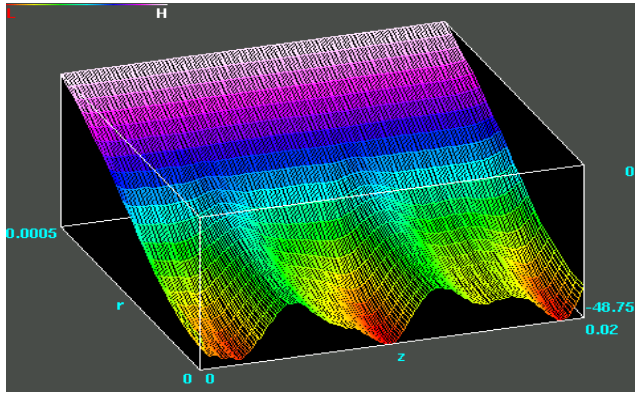

Particle in cell simulation of a 110 mA, 7.5 kV, 0.25 mm electron radius beam in a 0.5 mm radius grounded metal tubing as simulated with XOOPIC, in a PPM magnetic field with Bz = 0.33 T peak field.

Typical Focussing Magnets and Magnetic Field Configurations (I)

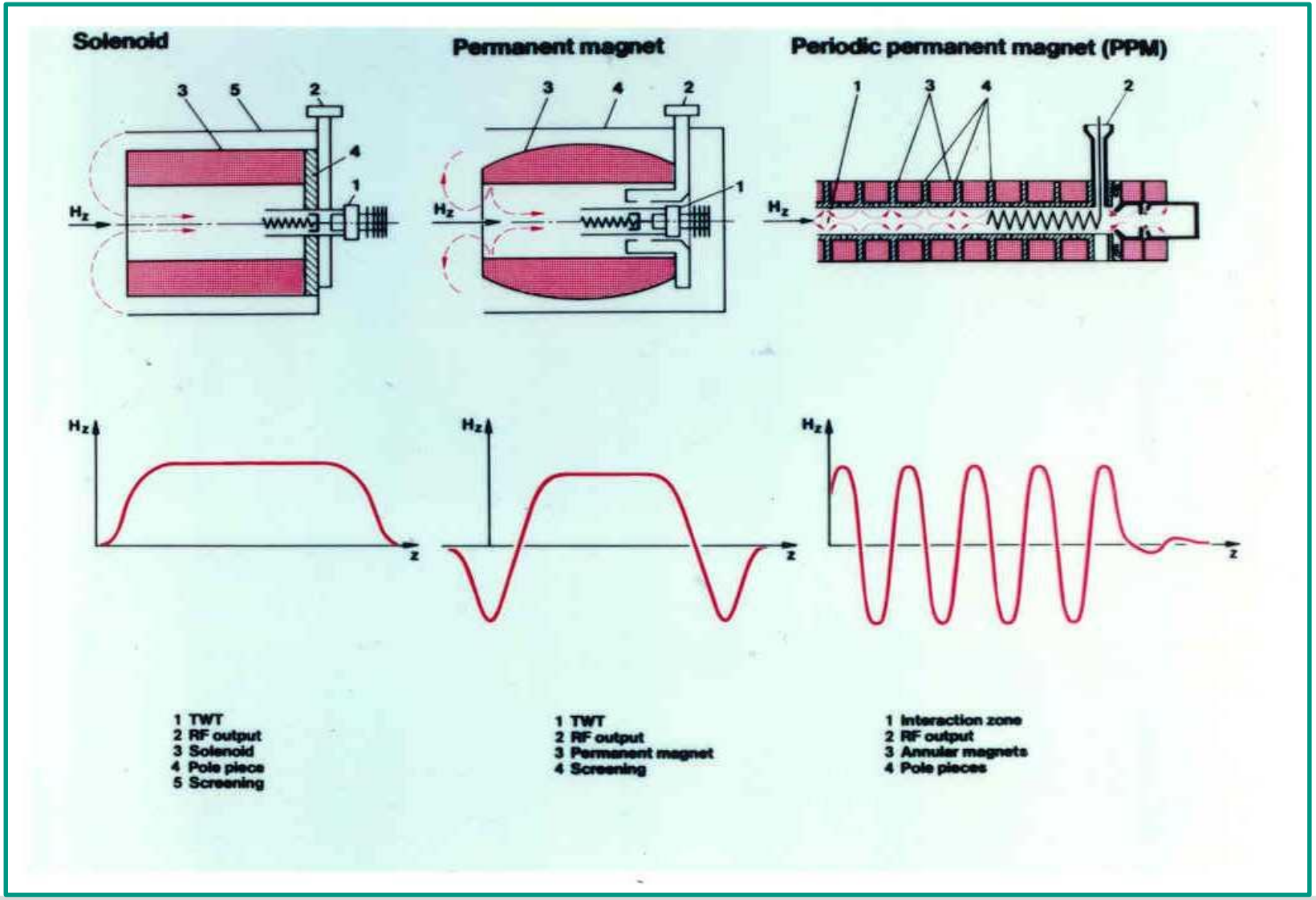

Typical Focussing Magnets and Magnetic Field Configurations (II)

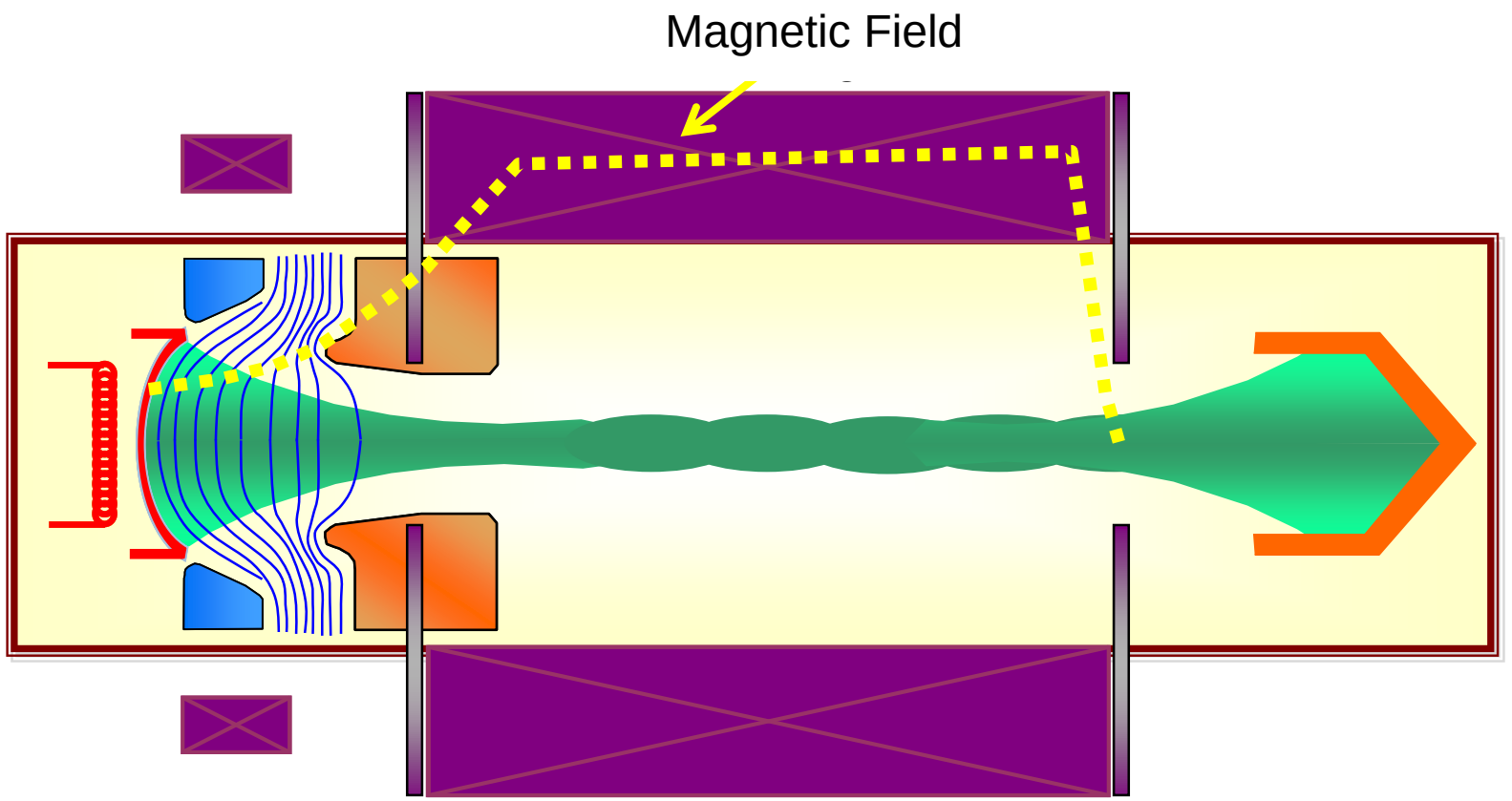

Typical Focussing Magnets and Magnetic Field Configurations (III)

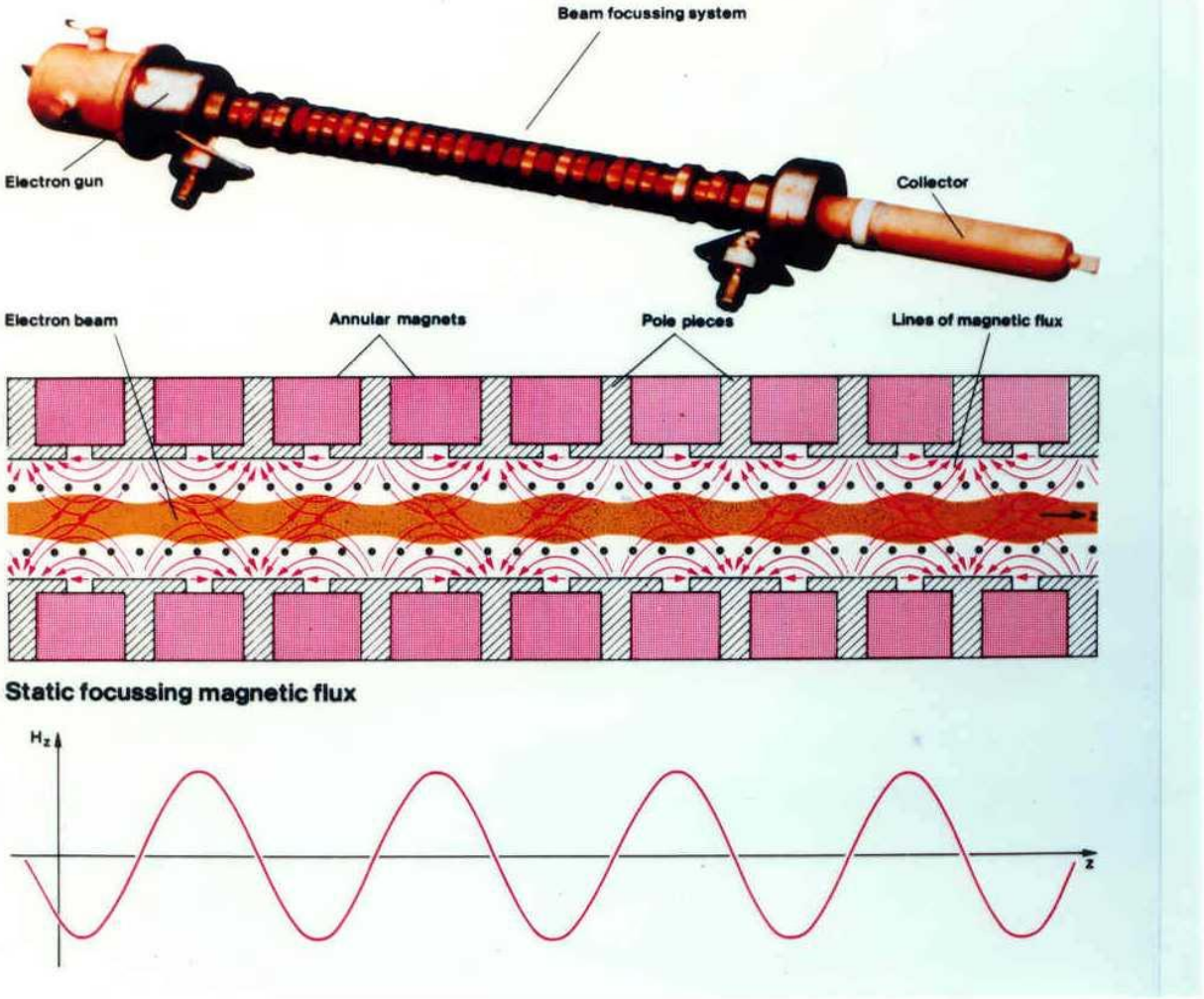

RF Input and Output

Coaxial Transmission Lines with integrated Dielectric Vacuum

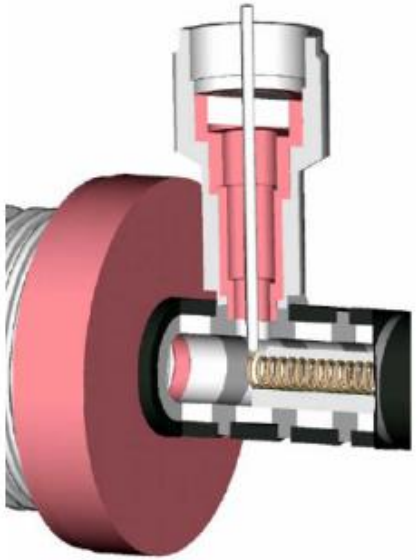

Input

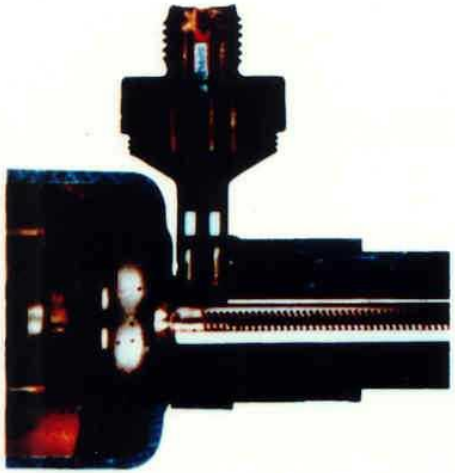

Output

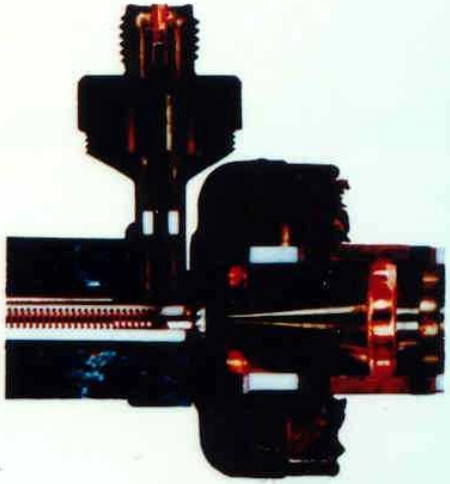

Waveguide transition to coupled-cavity delay line

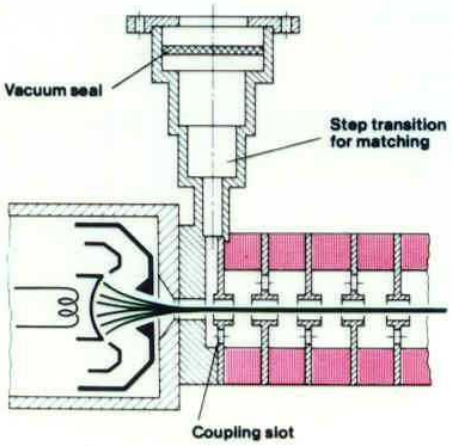

Coaxial transition from helix delay line

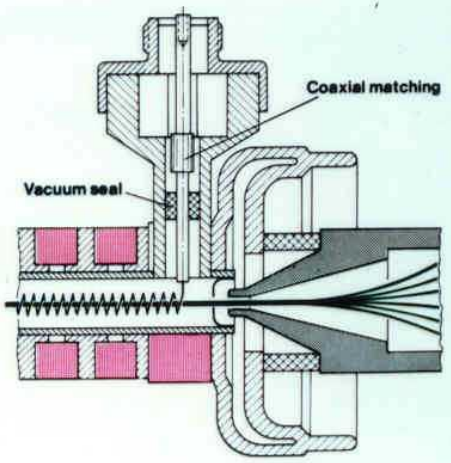

Collector Configurations

Electrostatically focused collector

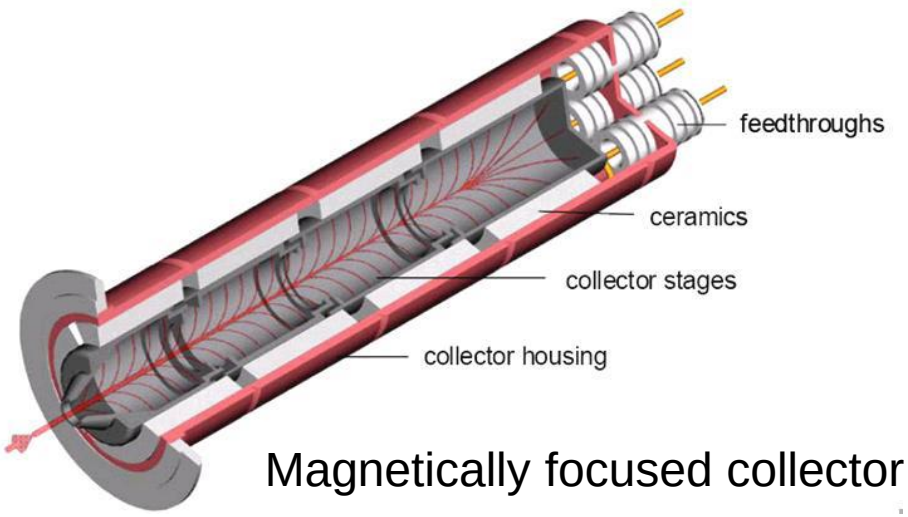

Magnetically focused collector

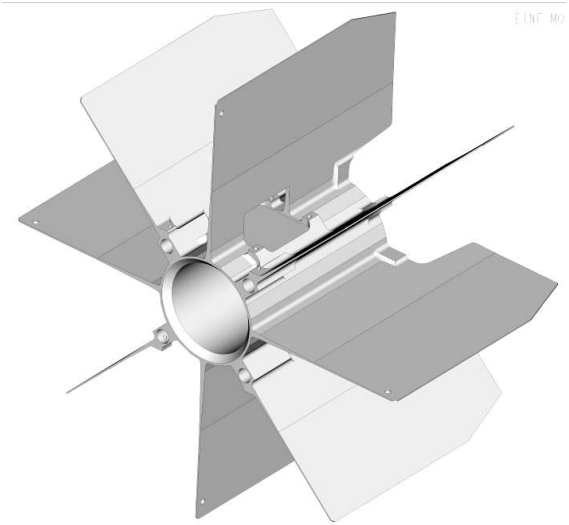

Radiator to be mounted on the surface of the collector (e.g. for space applications where the collector is positioned outside of the satellite)

Collector and Energy Recovery

Single-stage collector

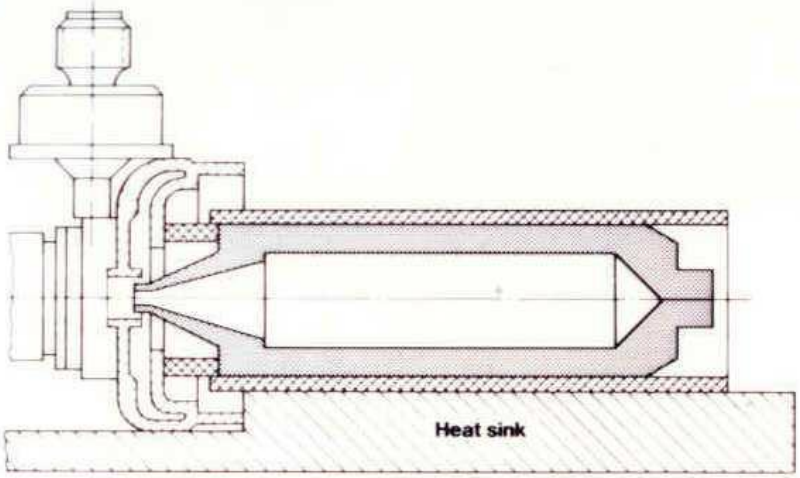

Electron velocity distribution

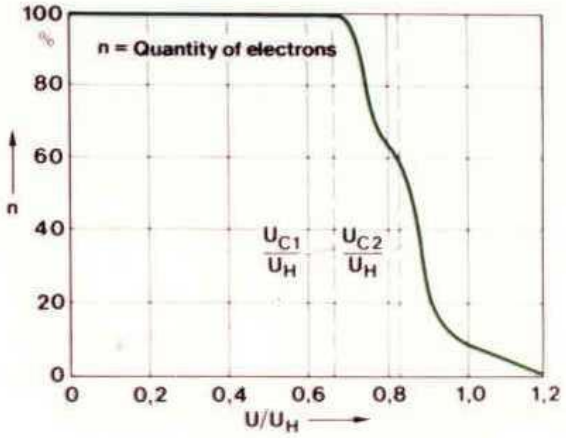

Double-stage collector (Single-stage depressed collector (SDC))

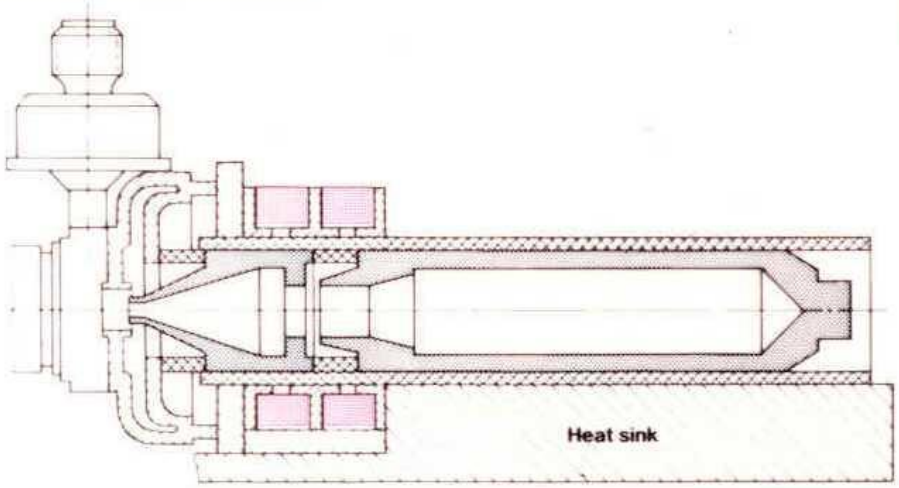

Efficiency, d.c. power and dissipated power for single and double-stage collectors

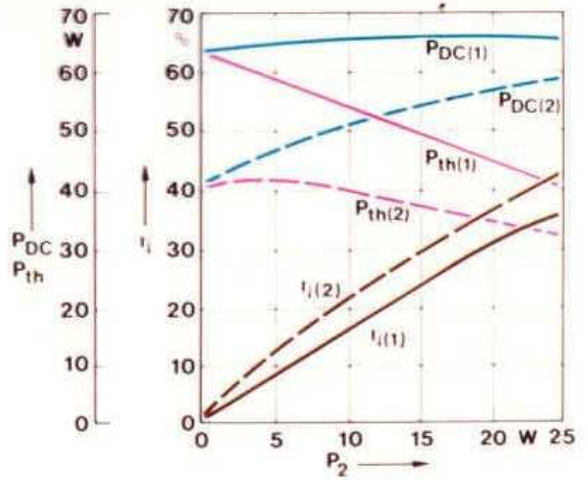

Electrostatically Focused Depressed Collector

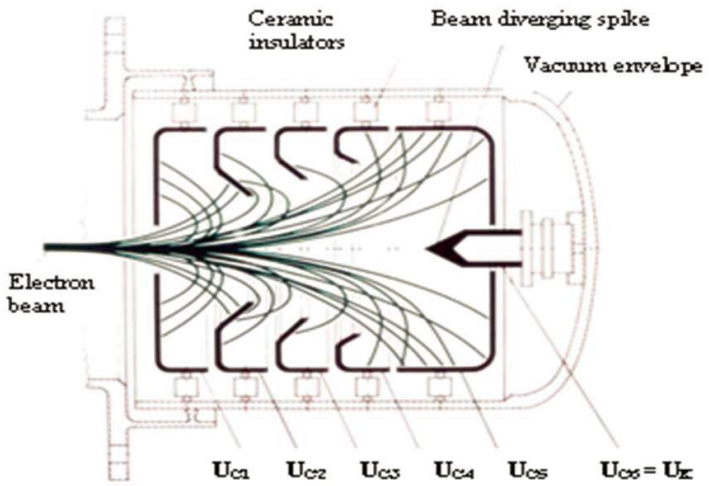

6-electrode collector
(5 stages + 1 spike on cathode potential)

250 W Space TWT TL 12250.

Efficiency 48%.

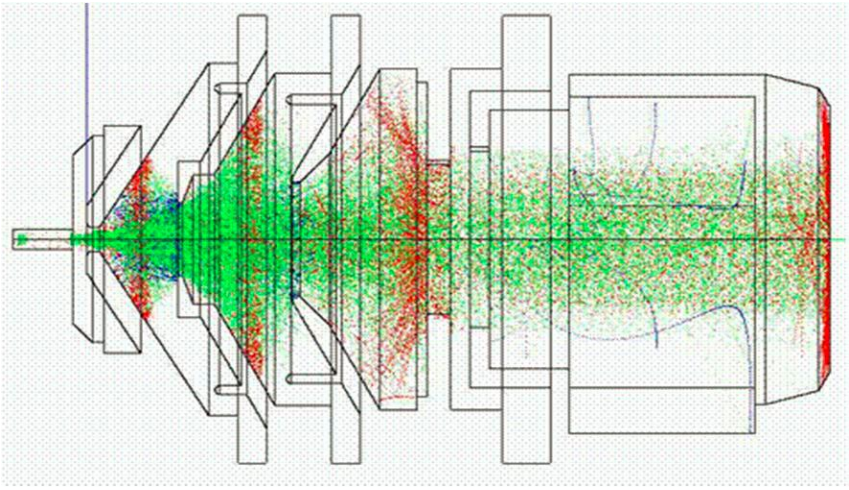

Primary electrons (green)
Reflected electrons (blue) and
Secondary electrons (red)
in electrostatically focused 4-stage collector.

Simulated with Thales Electron Devices PIC code Collect 3D

150 W Ku-band TWT (68% Efficiency).

Energy Recovery in 4-Stages Electrostatic Depressed Collector

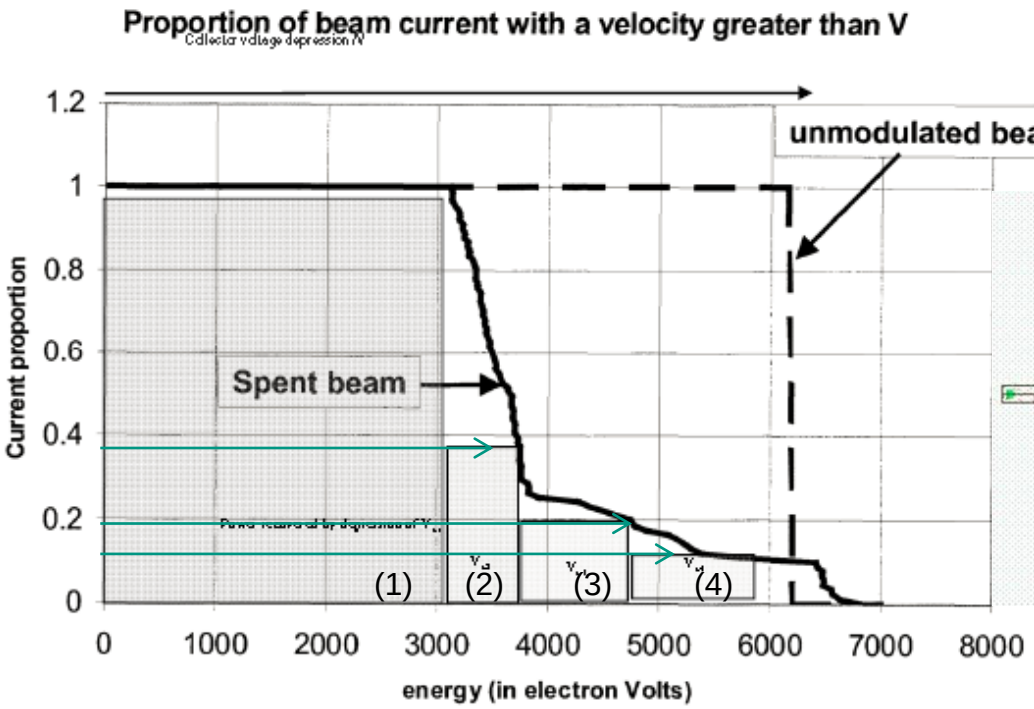

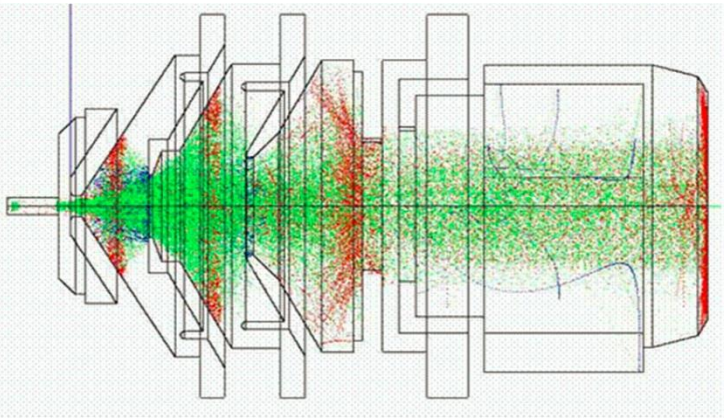

: Typical velocity/energy spectrum of the spent electron beam at the collector entrance and recovered power proportions (shaded area) of a Ku-band TWT with V_H = 6250 V, V_{C1} = 3250 V, V_{C2} = 2500 V, V_{C3} = 1750 V and V_{C4} = 450 V with respect to cathode. The collector efficiency is represented by the ratio of the shaded area to the total area below the spent beam distribution curve.

4-Stages Magnetically Focused Depressed Collector

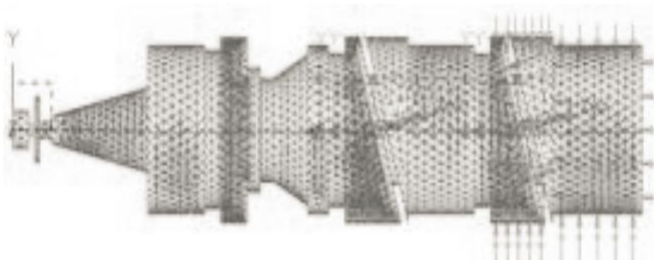

COLLECT3D VelizyMesh 20dB ibo Nunn 14.04.03

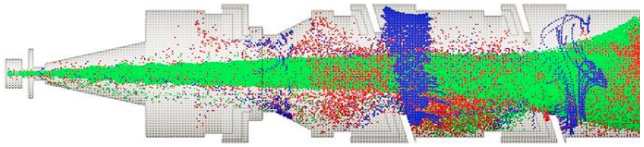

Without RF

Cliché No : 01/04 npart.: 170509 tps : 0.004167 ns

COLLECT3D VelizyMesh SAT Nunn 14.04.03

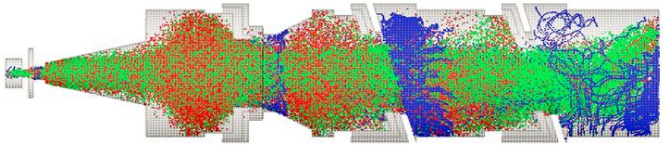

(1) (2) (3) (4)

Cliché No : 01/04 npart.: 245130 tps : 0.004167 ns

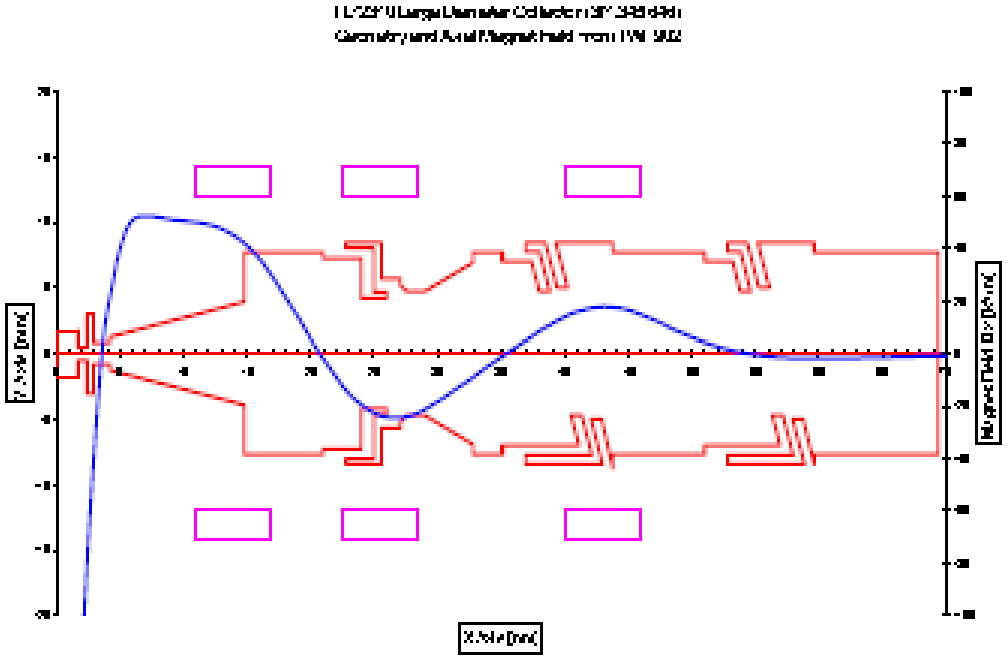

With RF (saturation)

Primary electrons (green)

Reflected electrons (blue)

Secondary electrons (red)

Example: 2-Stages Depressed Collector

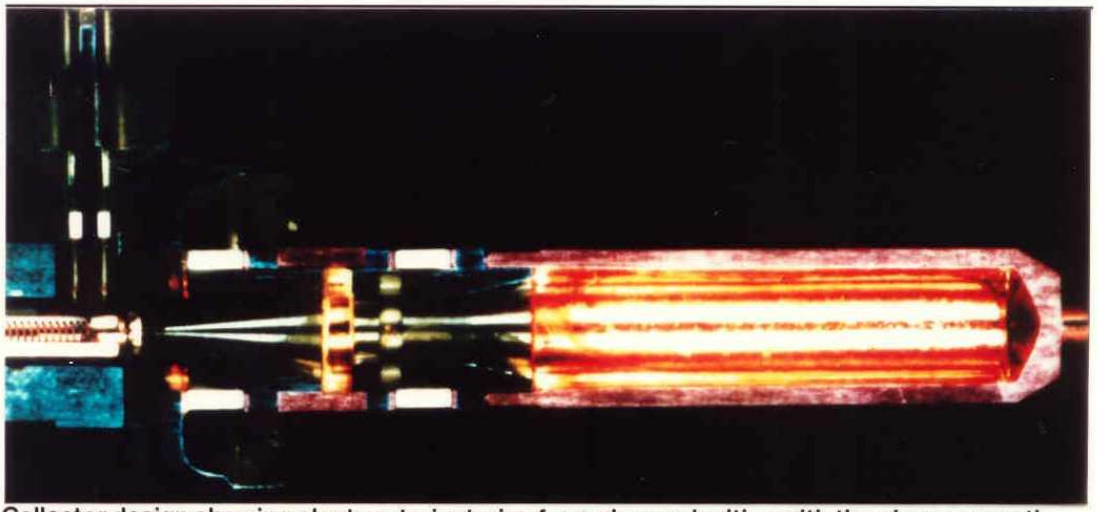

Collector design showing electron trajectories for various velocities with the given magnetic field distribution

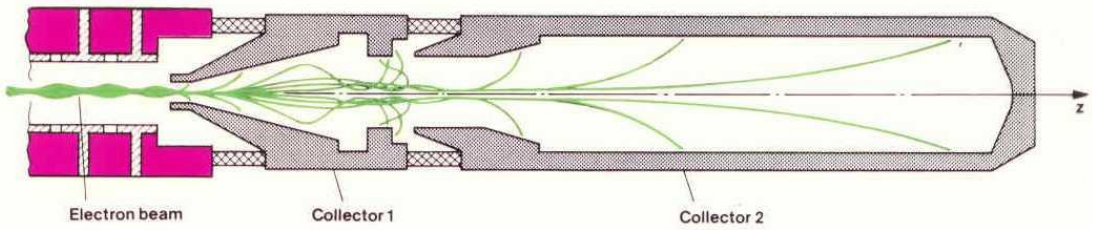

Static focussing magnetic field

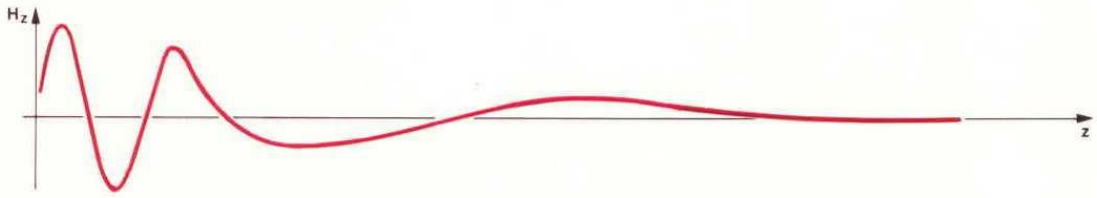

Different Multi-Stage Depressed Collectors

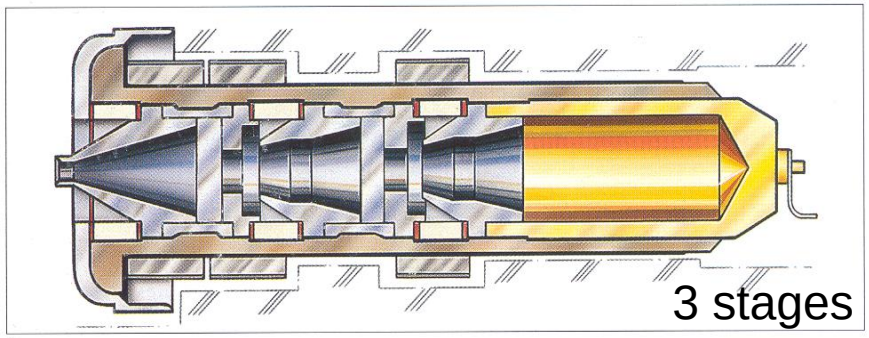

1

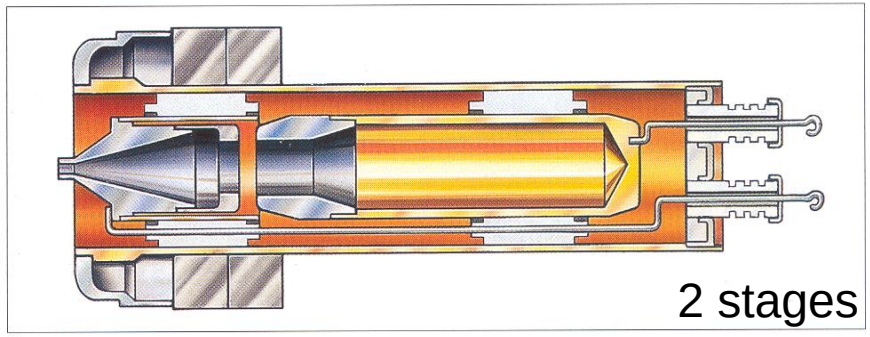

2

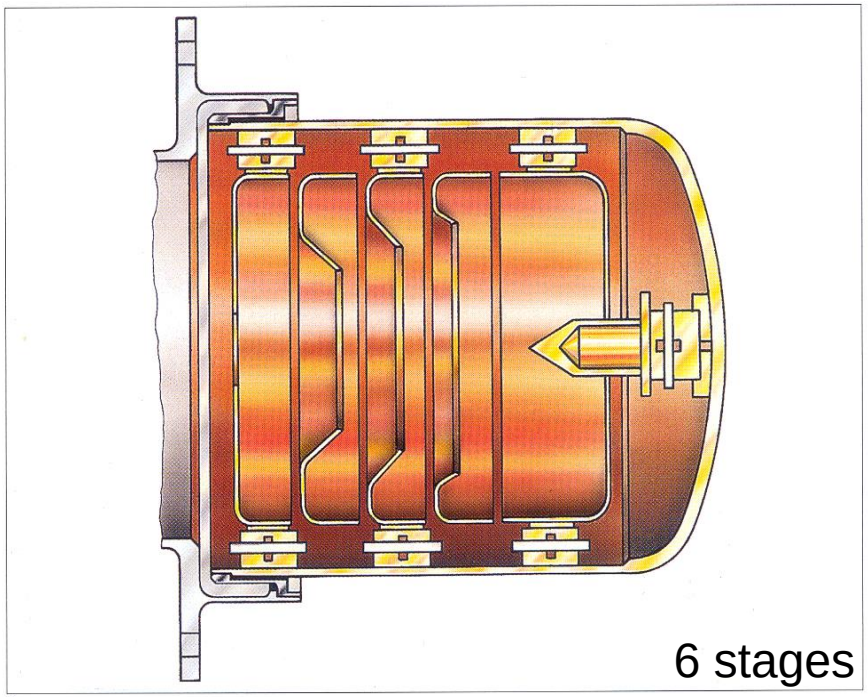

3

$$P_{C,diss} = \sum_i I_{Ci} \cdot V_{Ci} - P_2$$

The entrance condition for the residual kinetic energy of electrons in stage *i* is related to the increase of potential energy of electrons entering the stage *i*+1

Simulation Calculations on a 3-Stage Depressed Collector

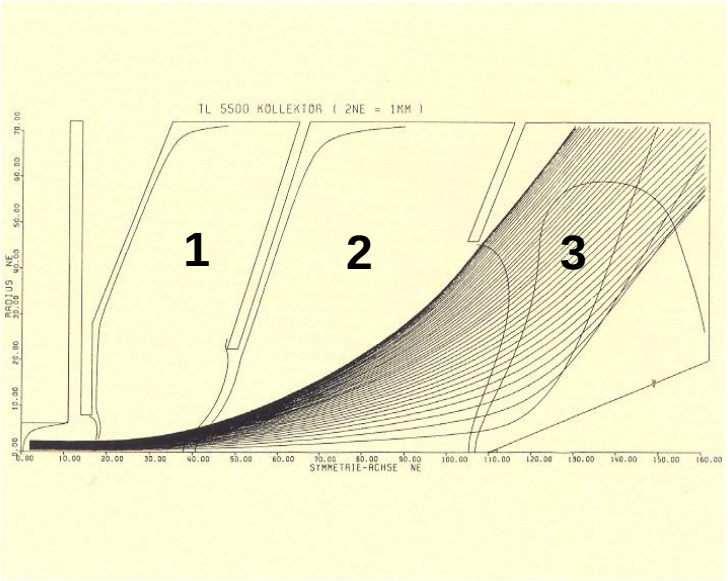

Zero drive: non-modulated e-beam

All electrons reach the 3rd stage

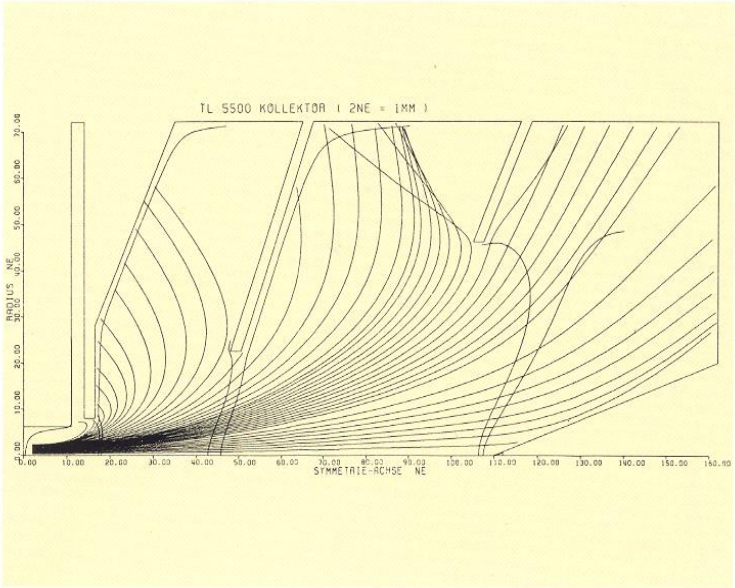

Saturated gain: maximum modulation of e-beam

All 3 stages catch electrons

Multi-Stage Depressed Collector (4 Stages) for Relativistic Beam Device

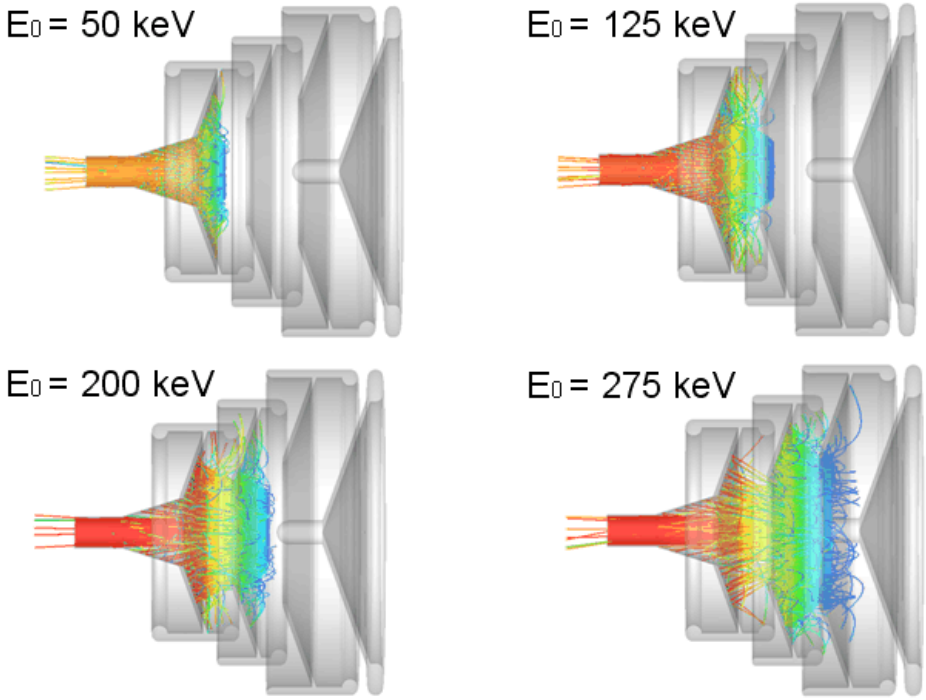

Beam trajectories for 4 different initial energies simulated with CST PS.

Depressed Collector with four different initial beam energies.
CST Particle Studio Simulations (M.J. de Loos et al. Pulsar Physics)

Relation between TWT Total-, Beam- and Collector Efficiency (I)

The total efficiency η_{tot} and the beam power efficiency η_{beam} (or basic efficiency η_0) of a TWT can be simply defined and rewritten as:

$$\eta_{tot} = \frac{P_{fund}}{P_{el}} = \frac{\eta_{beam} \cdot P_{beam}}{P_{RF} + P_{losses}} = \frac{\eta_{beam} \cdot P_{beam}}{P_{beam} - (P_{beam} - P_{RF} - P_{losses})}$$

where P_{fund} is the fundamental frequency RF power at the TWT output and P_{RF} is the total RF power (including fundamental and harmonic RF power and RF losses). $P_{beam} = V_H \cdot I_K$ is the electron beam power and P_{losses} are the thermal losses produced in the tube, respectively. A short analysis of the thermal TWT losses P_{losses} provides:

$$P_{losses} = P_{Coll,losses} + P_{H,therm} + P_{A,therm} + (P_{filament})$$

Neglecting the small quantities filament power, helix and anode losses, the term $P_{recover} = (P_{beam} - P_{RF} - P_{losses})$ becomes approximately equivalent to the recovered kinetic electron beam power by reduced collector voltages. With the definition of the collector efficiency η_C as the ratio of the recovered power to the entering beam power

$$\eta_C = \frac{P_{recover}}{P_{enter}} = \frac{(P_{beam} - P_{RF} - P_{losses})}{P_{beam} - P_{RF}}$$

we get a simplified relation between total, beam power and collector efficiency by further neglecting the harmonic power and the RF losses in P_{RF} and by division with P_{beam}:

$$\eta_{tot} = \frac{P_{fund}}{P_{el}} = \frac{\eta_{beam} \cdot P_{beam}}{P_{beam} - \eta_C (P_{beam} - P_{RF})} = \frac{\eta_{beam}}{1 - \eta_C (1 - \eta_{beam})}$$

Relation between TWT
Total-, Beam- and Collector Efficiency (II)

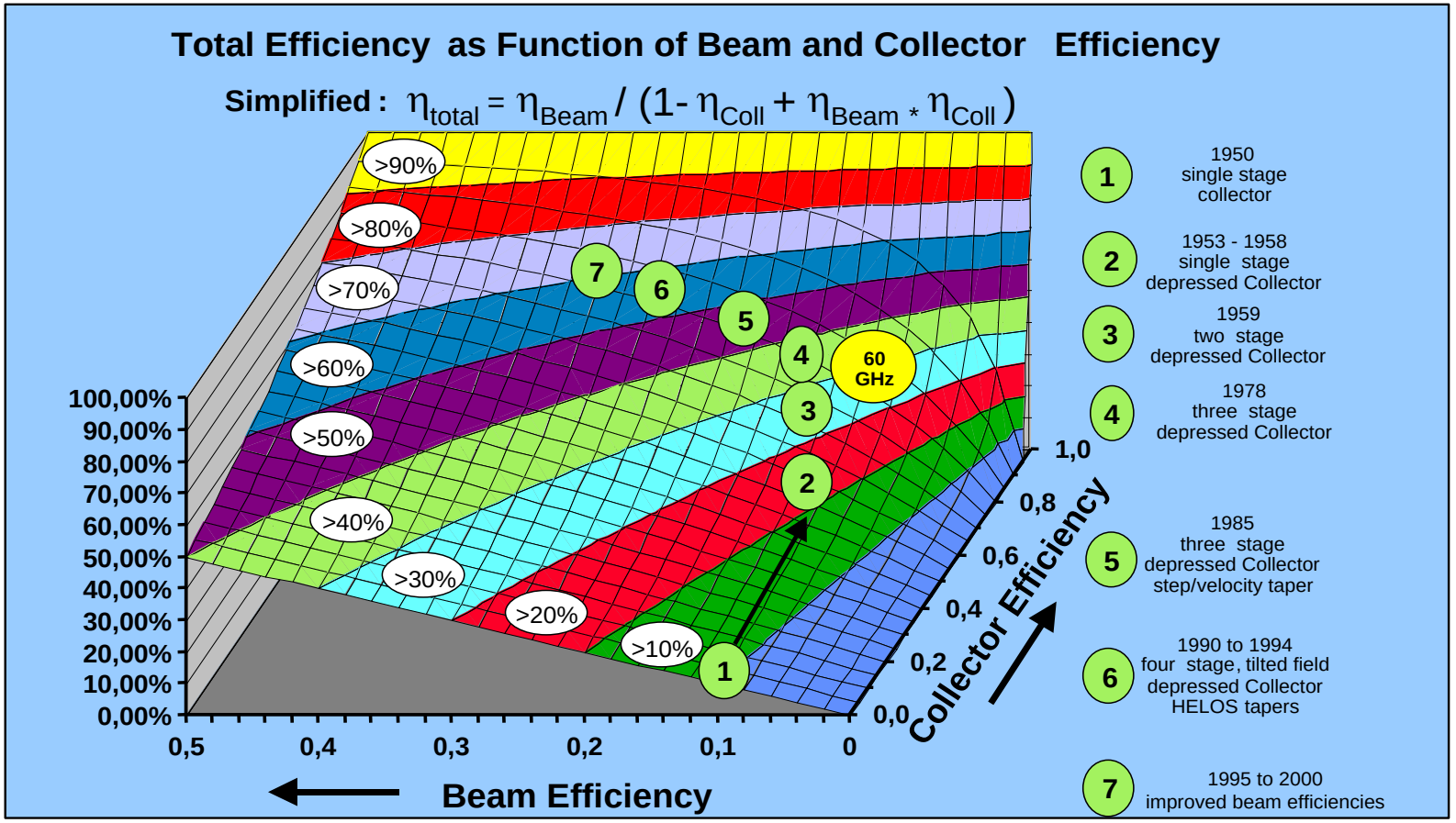

Total efficiency as function of the two variables beam efficiency and collector efficiency. The historical path from single-stage collector tubes (point 1, efficiency = 10%) to 4-stage tilted field collector tubes with enhanced beam efficiency (point 7, efficiency = 70%) is sketched for Ku band TWTs.

Loss Analysis of a Typical Ku-Band Space TWT

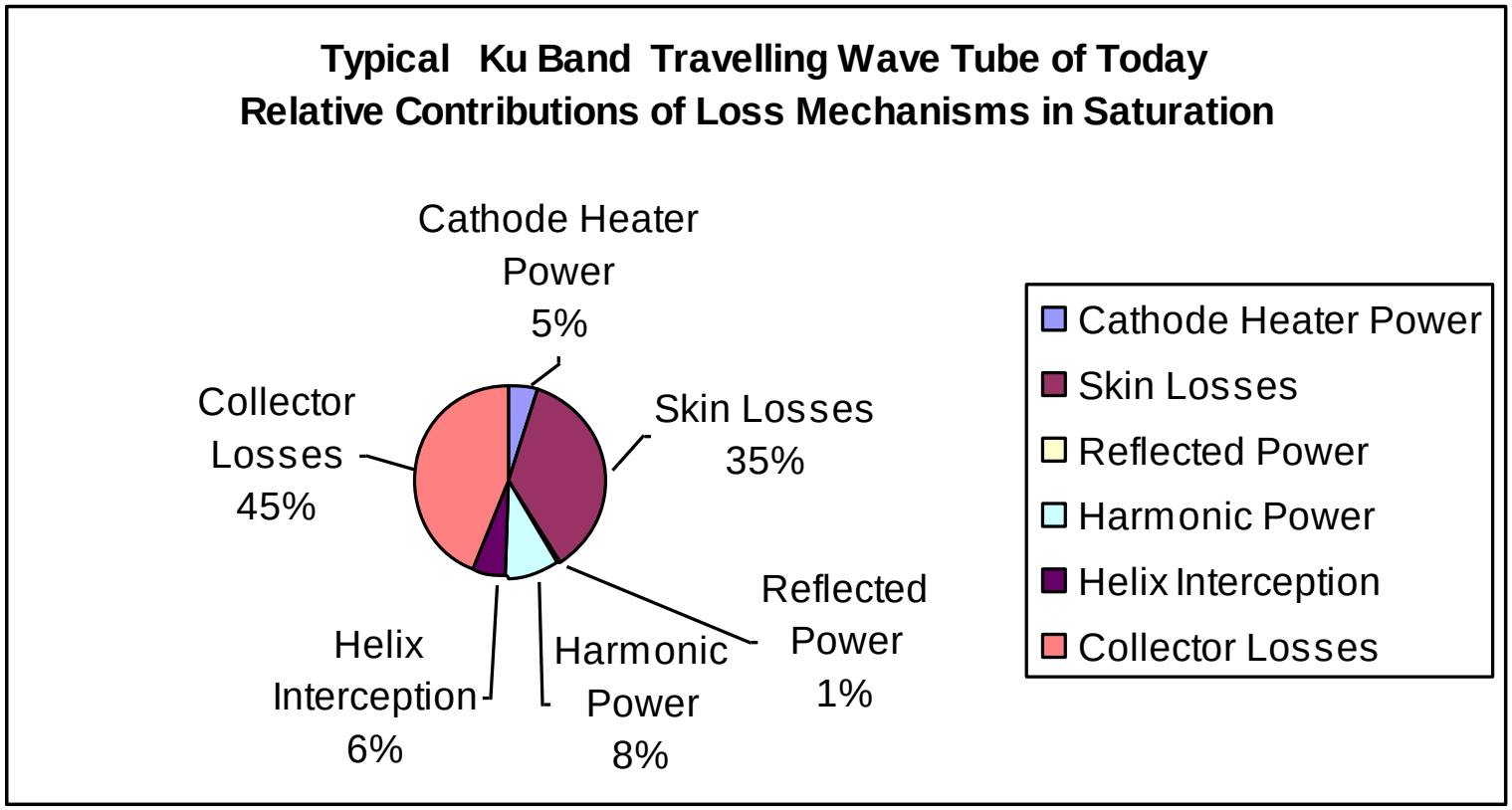

Total distribution of thermal losses in a modern TWT

TESAT – Company in Germany
Satellite „Payloads“ with TWTAs

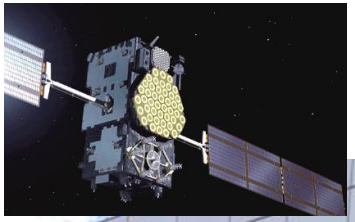

Dual TWT amplifier

- TESAT is the global market leader with approx. 50 % market share
- Outstanding production capacity (e.g. with robotic assembly) with highest quality
- High test automation and comprehensive testing facilities (e.g. 33 vacuum chambers)
- Lifetime in orbit of over 18 years
- ESA qualified PCB manufacturer / ESA qualified hybrid manufacturer

View into TESAT’s manufacturing building

Location	**Backnang, Germany**
Core business	Spacecom Satellite Payload, Equipment & Subsystems
Employees 2011	1200
Turnover 2011	227 Mio. Euro
Equipment Capacity	Up to 1500 Units per Year
Programs	Up to 75 per year
Homepage	www.tesat.de

Principle of Typical Satellite „Payload“

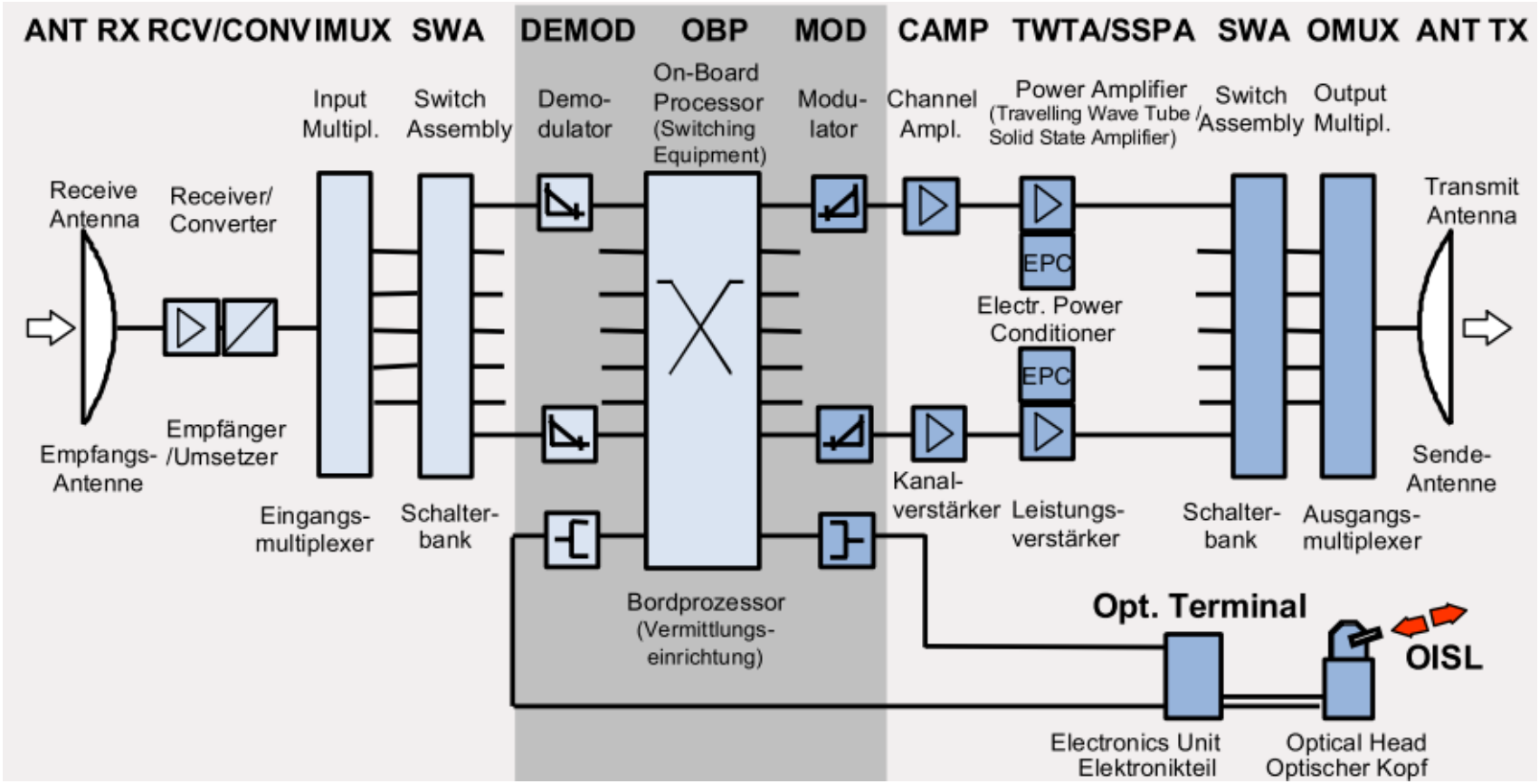

Input section Data processing units Output section

TWTA (TWT Amplifier) Scheme (7 Channels)

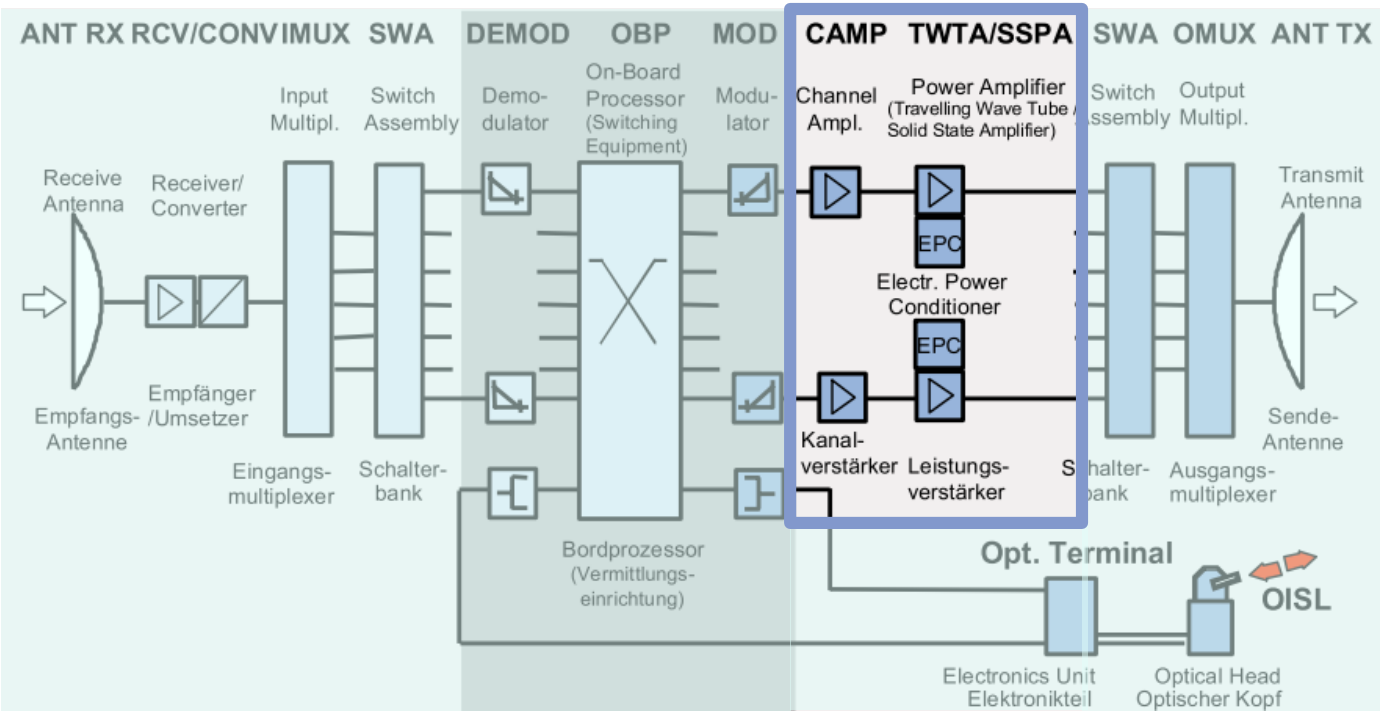

The TWTA assembly is located within the output section of a satellite communication payload.

Its main objective is the power amplification of the RF-signal which was generated by the modulator unit.

Example: Ku-Band TWTA

Ku-Band TWTA

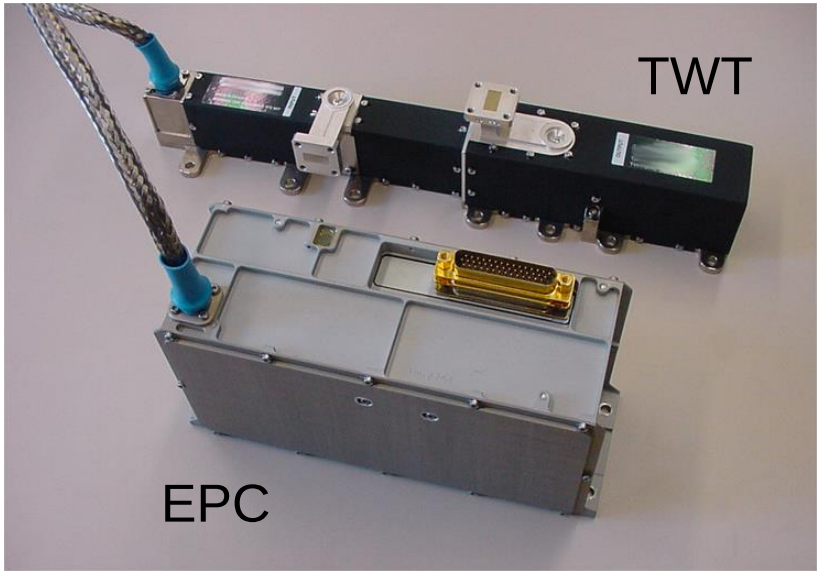

“Electronic Power Conditioner (EPC)”,

Typical Ku-Band TWT Parameters	
Frequency:	10.7 to 12.75 GHz
RF-input:	-10 to 0 dBm
RF-output:	> 100 W
Gain:	50 to 60 dB
Phase shift:	Up to 50° to 55°
Efficiency:	Up to 70 %
DC-voltages:	Supply voltages up to 7 kV from EPC

Typical Ku-Band EPC parameters	
DC-input:	var. 50 V / 60 V / 100 V from satellite
Output power:	Up to 350W (depending on TWT and requirements)
DC-output	Supply voltages towards TWT up to 7 kV
Efficiency:	Up to 94 %

TWTA: Typical Characteristics AM-AM

Output power vs. Input drive (AM-AM transfer)

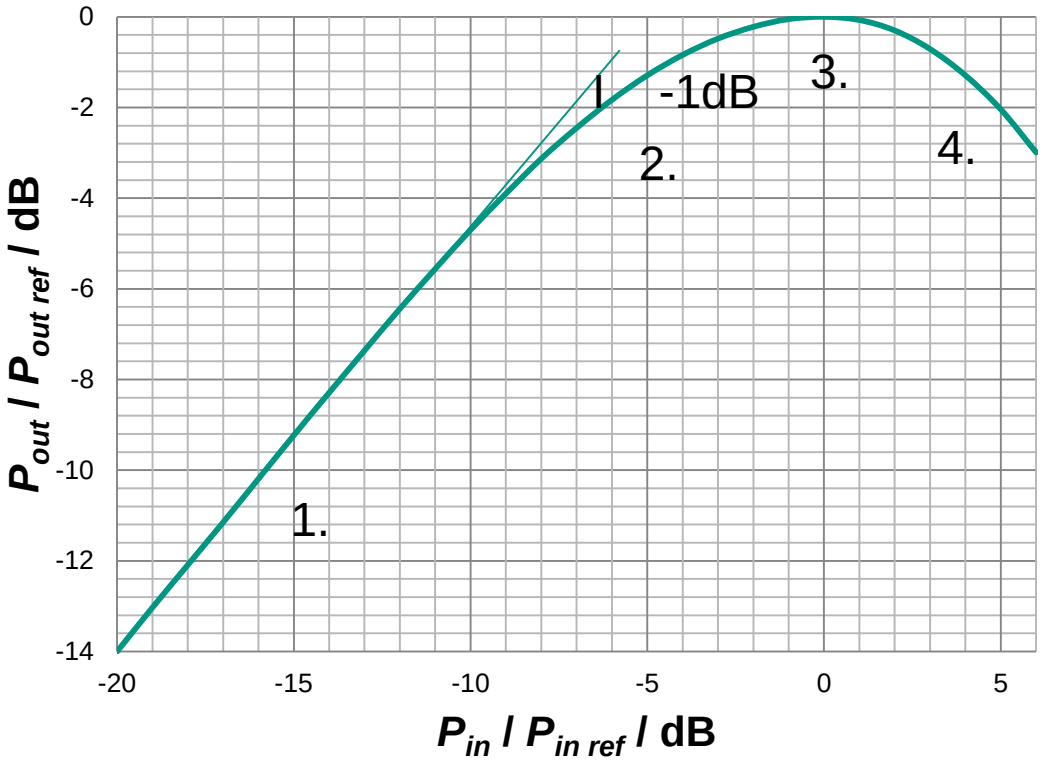

1. Linear regime
2. Compression regime
3. Saturation point
4. Overdrive regime

Relation between input- and output power is linear only up to the compression zone of the amplifier (- 1dB compression point).

TWTA: Typical Characteristics AM-PM

Phase shift vs. input drive (AM-PM transfer)

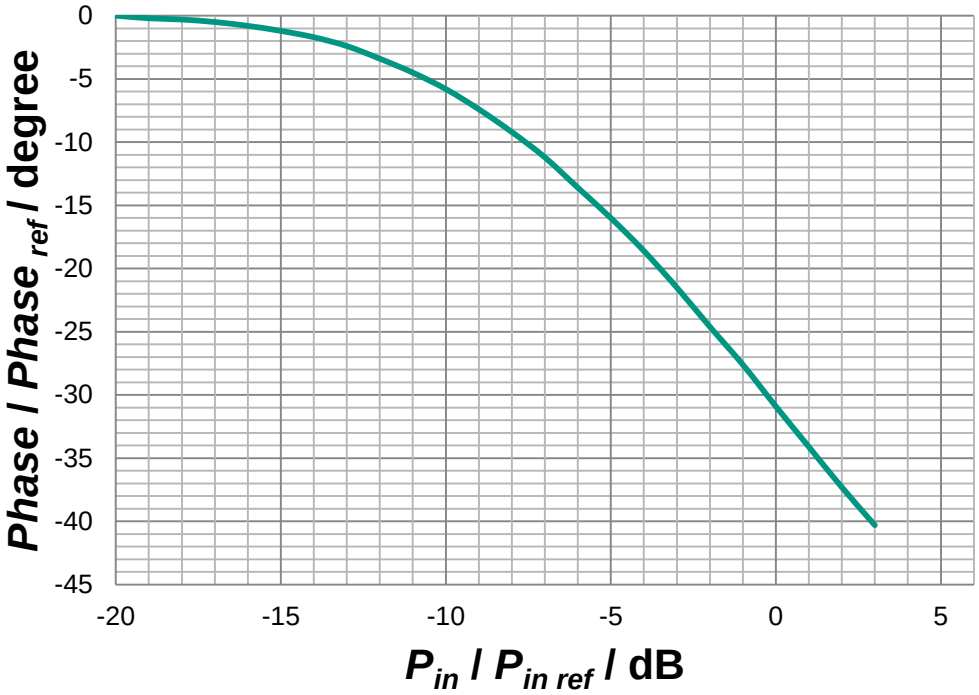

The phase of the output RF-signal is not constant at different input drive levels.

This behavior is not favorable depending on the utilized modulation scheme and can be compensated by a linearizer (linearized channel amplifier LCAMP).

Definition: Hybrid Microwave Power Module (MPM)

A hybrid microwave power module (MPM) consists of three functional units:

1. **Travelling Wave Tube (TWT)**, as high power RF amplification unit
2. **The Linearized Channel Amplifier (LCAMP),** which acts as a RF pre-amplifier and linearizer
3. **Electronic Power Conditioner (EPC),** which is the DC power converter/supply for the TWT

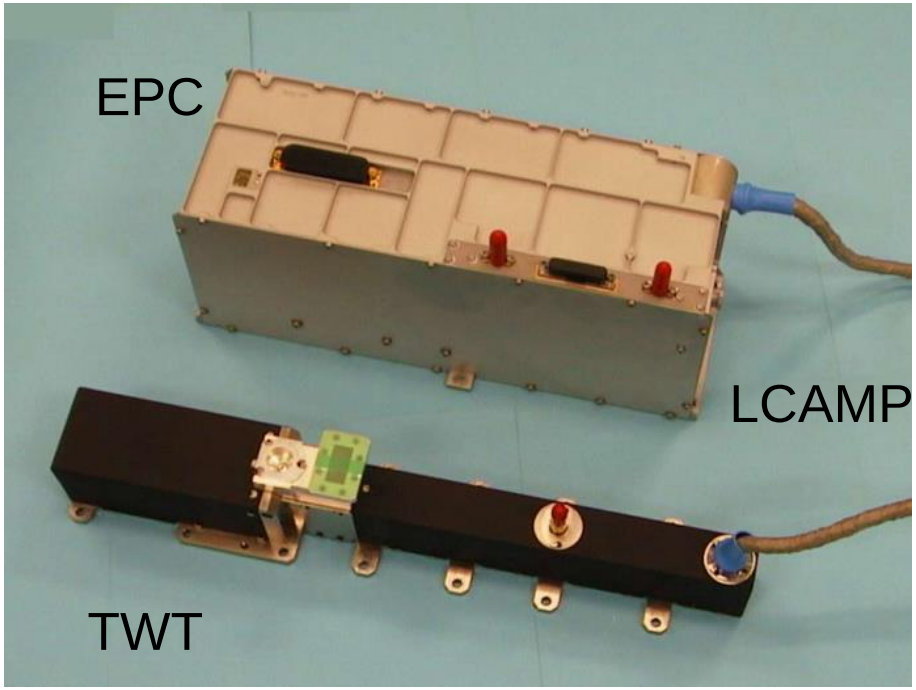

Ku-Band MPM
(LCAMP and EPC in one housing, here TWT not integrated)

Real Microwave Power Module (MPM)

All included (TWT also)!

TMD

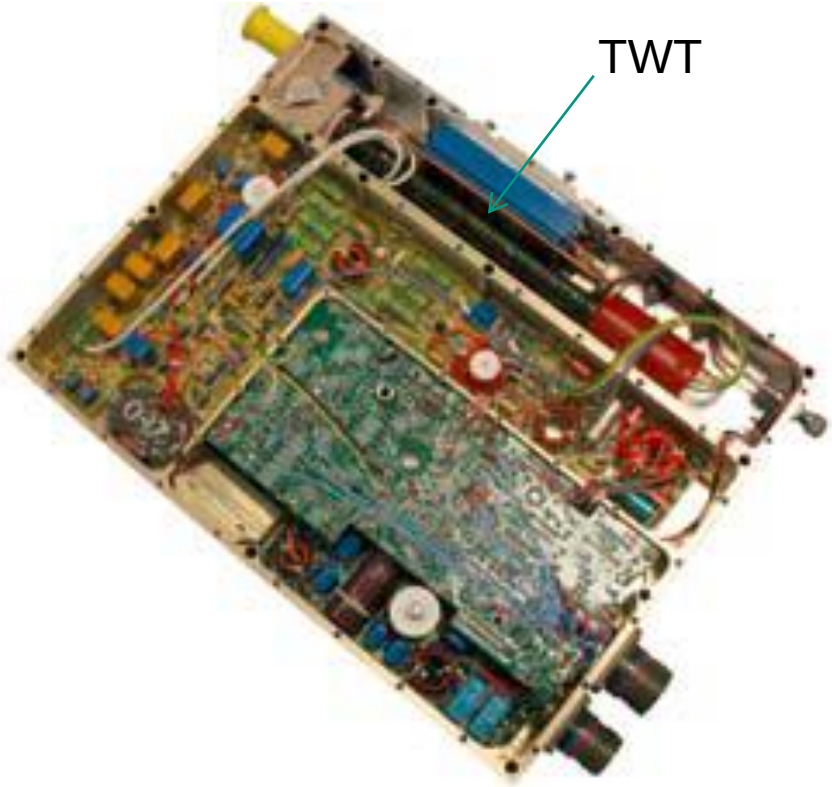

Dual Hybrid MPM

Within a dual hybrid MPM, one EPC feeds two TWTs (safes weight and space on satellite).

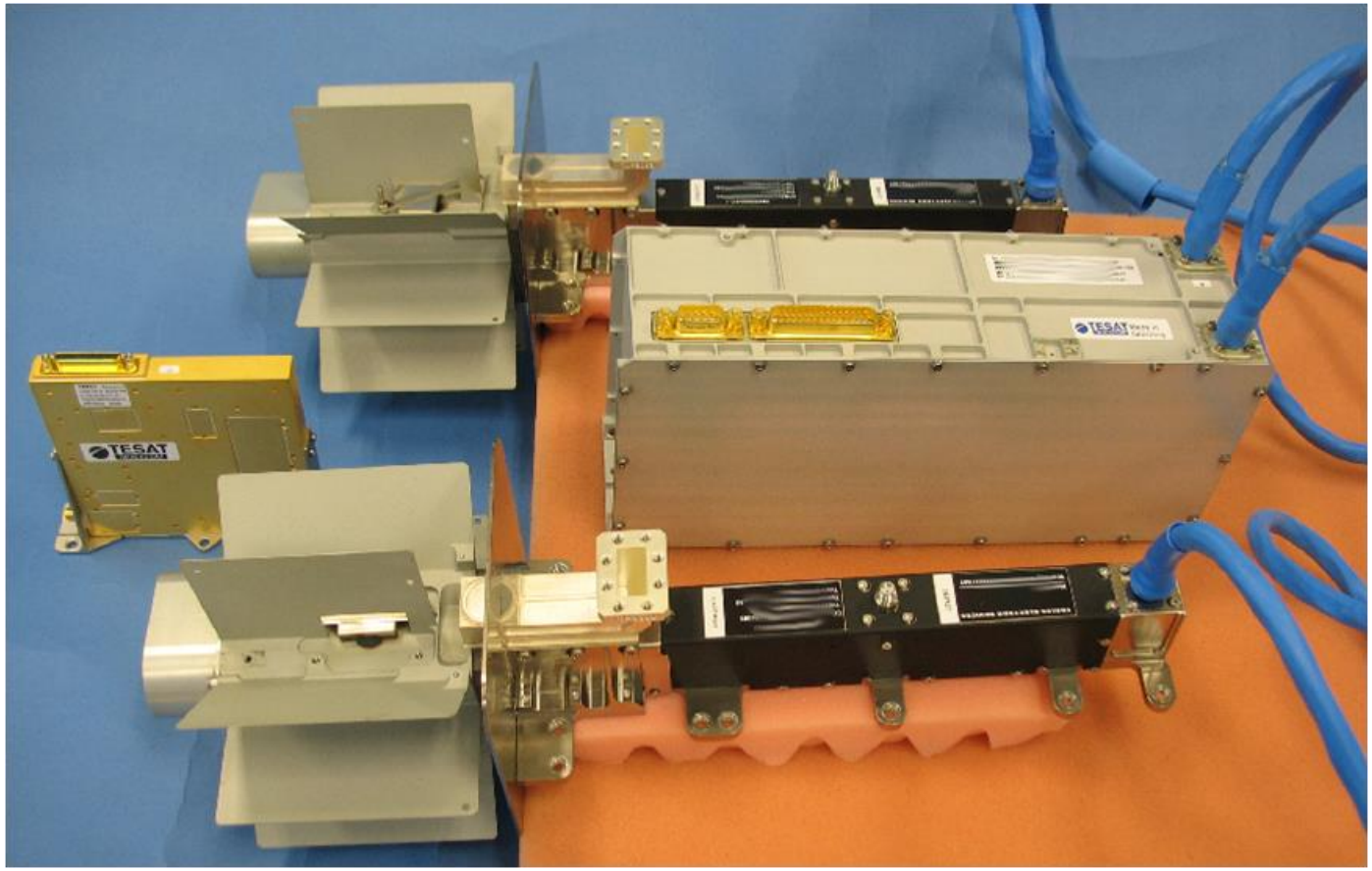

Definition: LCAMP

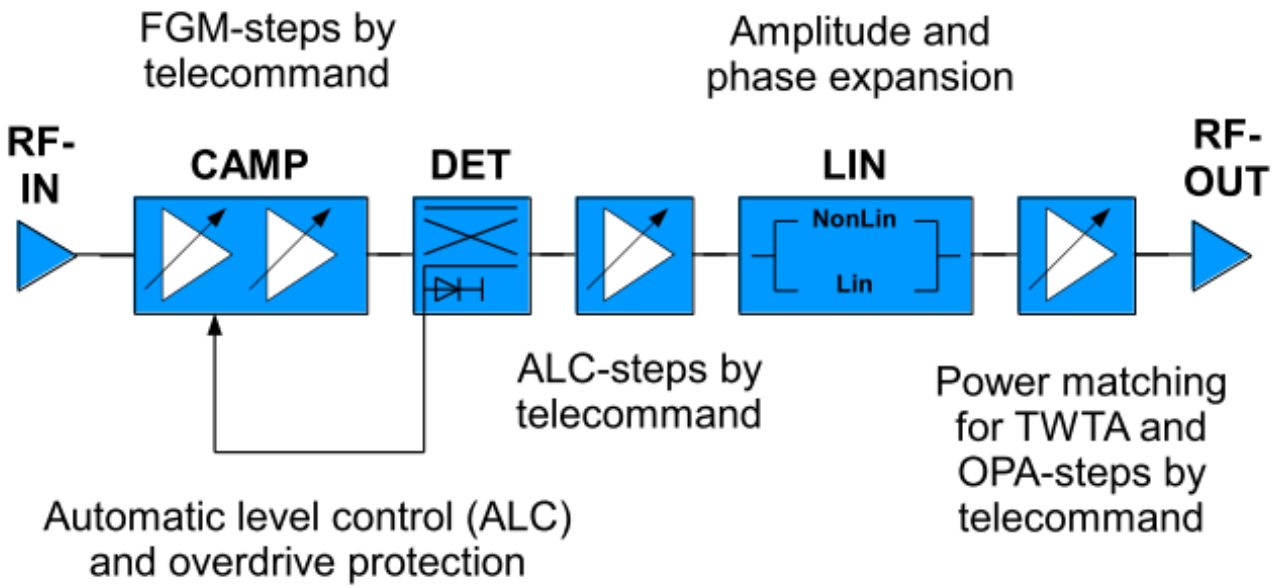

The LCAMP consists of the following functional blocks:

- The channel amplifier (CAMP) at the beginning of the RF-chain
- Automatic Level Control (ALC) and Power Matching
- The Linearizer (LIN) towards the end of the RF chain

Modern LCAMP offer several different operating modes, which give the satellite operator the possibility to tune the RF-signal as needed and to compensate drifts over lifetime.

LCAMP: Channel Amplifier

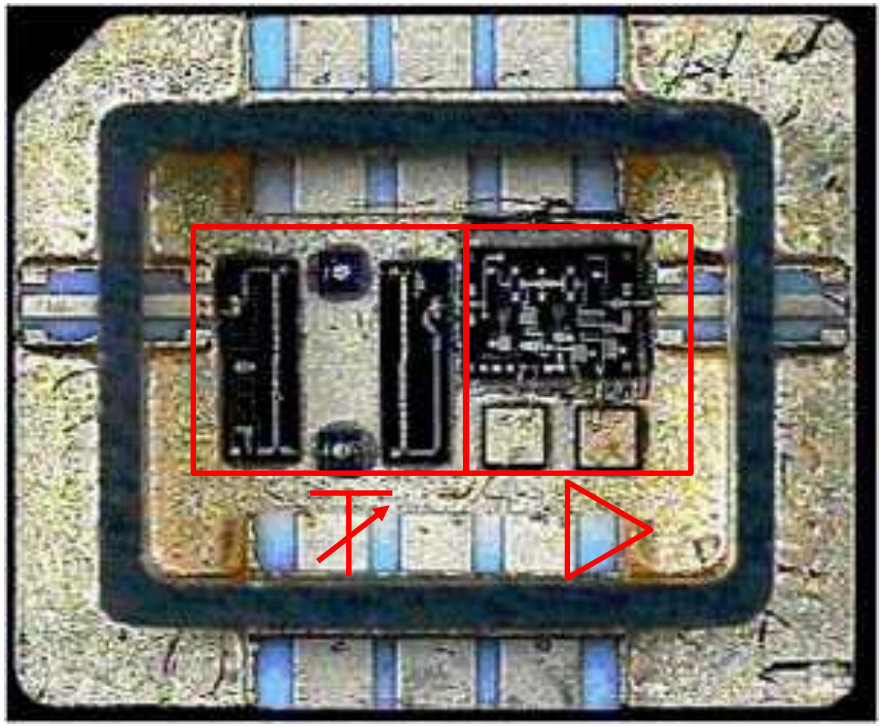

The channel amplifier section consists of several Variable Gain Amplifier hybrids (VGAs). These VGAs are universal gain blocks consisting of a PIN-diode attenuator stage to adjust the gain level followed by an amplifier stage.

LCAMP: Linearizer - Principle

With a tailored signal pre-distortion at the input of the TWT, the disadvantages of the TWT's characteristics can be compensated towards an ideal amplifier.

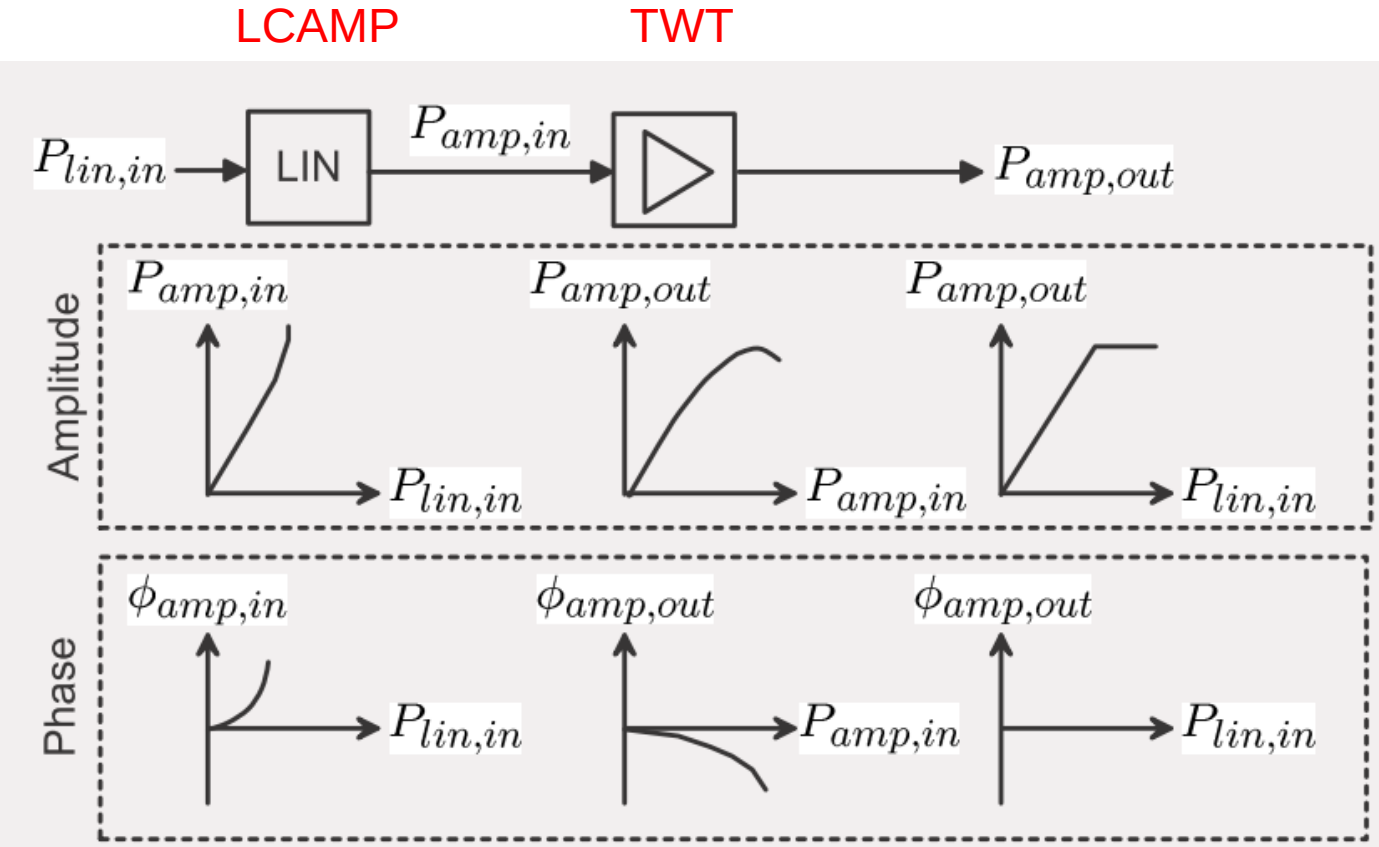

LCAMP: Linearizer

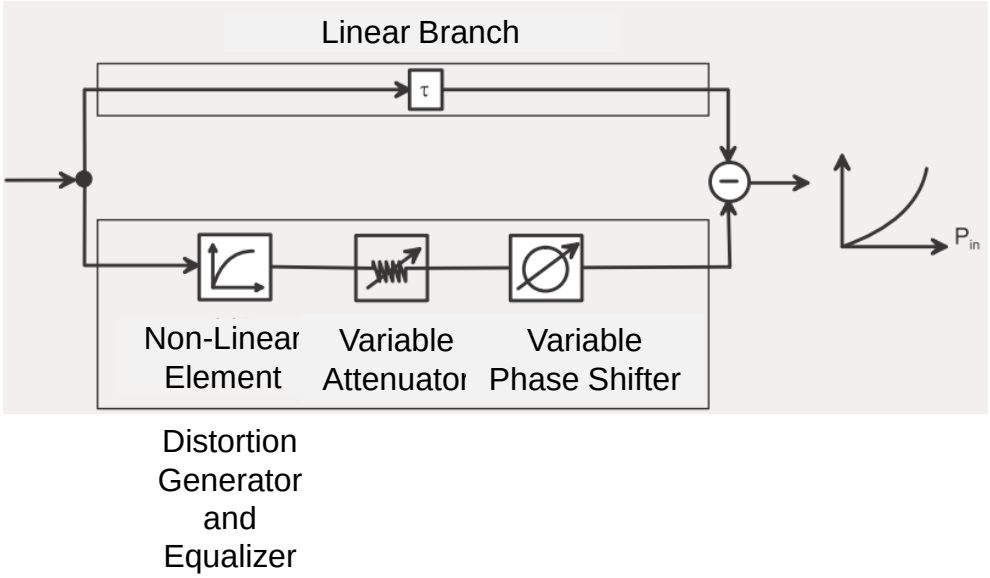

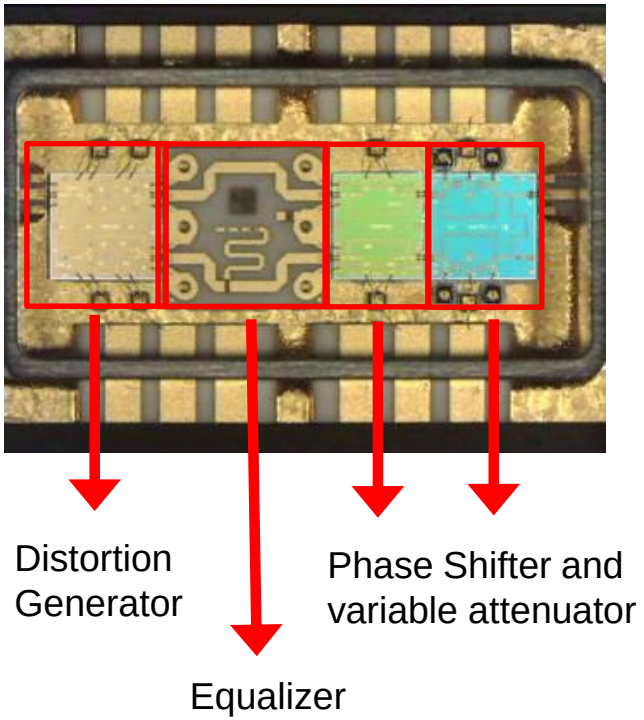

- The Linearizer can be subdivided into linear and non-linear branch
- The equalizer within the non-linear branch optimizes the characteristics over frequency
- Schottky diodes are utilized within the distortion generator as non-linear elements
- Varactor diodes are employed within the phase shifter

MPM: Setup with LCAMP

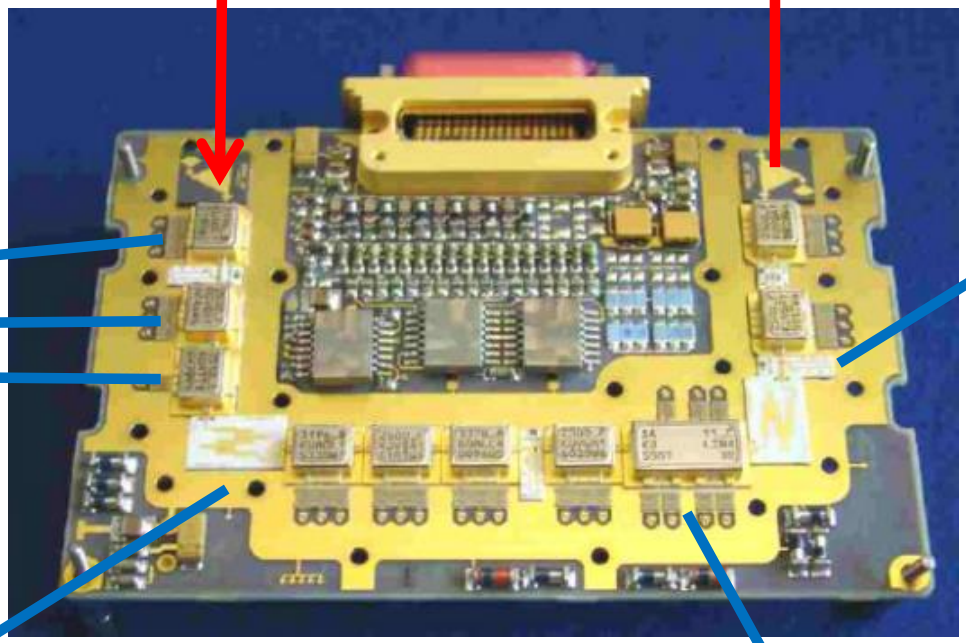

Definition: EPC

Primary functions:

• Highly efficient generation of high voltages for the TWT (up to 10 kV) from slightly variable and low voltage main bus (30 V to 100 V) of the spacecraft.

Secondary functions:

• Matching the telecommand interface of the spacecraft
• Generation of internal processes based on customer/mission requirements
• Protective circuits to protect TWT from incorrect operation
• Generation of secondary supply voltage towards LCAMP

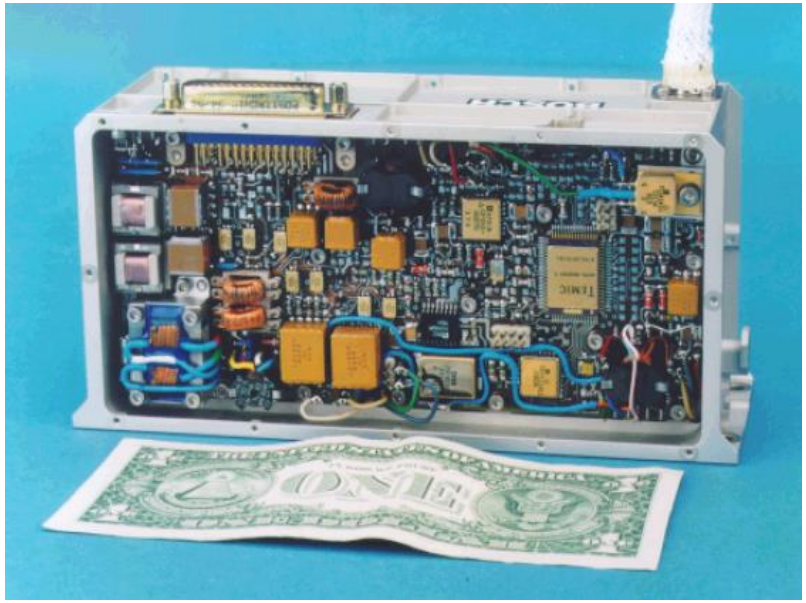

Voltage Supply for TWT

TWTs require usually the following voltages (relative to cathode voltage):

- Filament voltage U_F
- Wehnelt electrode voltage U_W
- Anode voltage U_A
- Helix voltage U_H
- Different collector voltages U_{C1} to U_{C4}

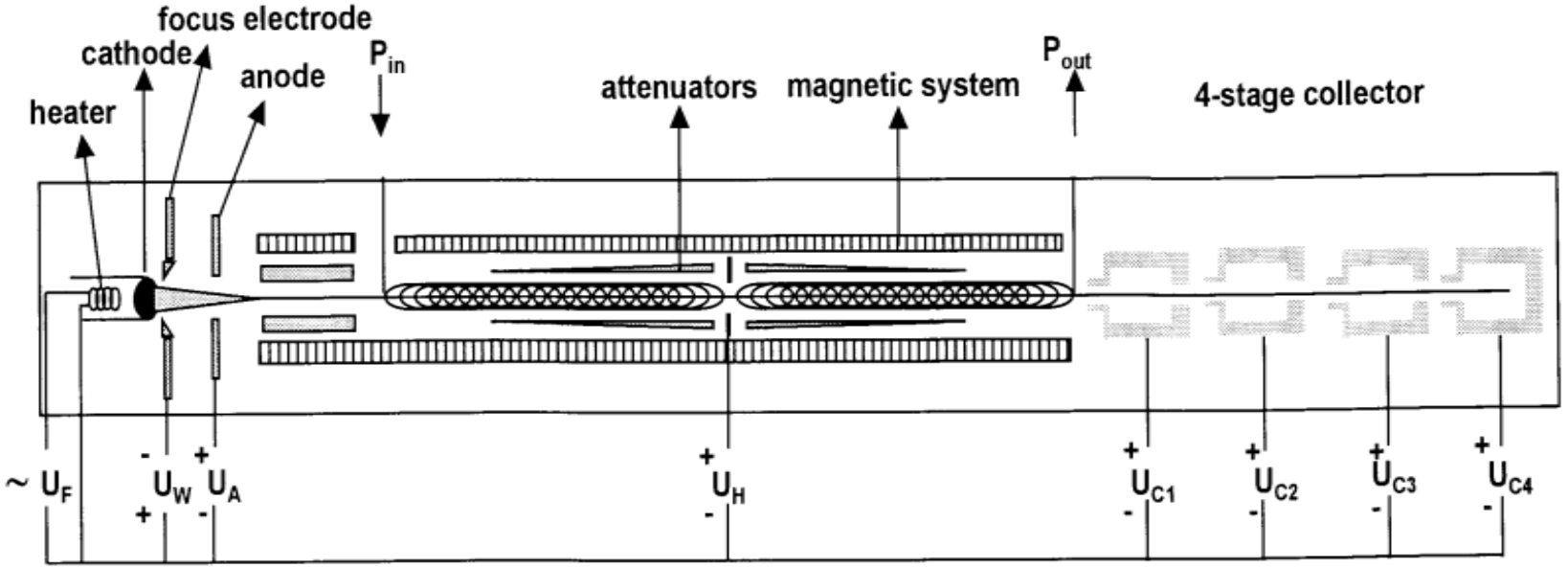

EPC – Schematic

The function and internal processes of the EPC, can be subdivided into 14 functional blocks:

- Input filter
- Pre-regulator with start-up regulator
- Digital control circuit
- Telemetry/tele-command interface
- Pre-regulator
- Power converter
- Auxiliary converter
- Secondary power supply
- Filament converter
- Filament voltage generation
- High voltage generation
- Helix voltage regulator
- Cathode control regulator
- Output filter

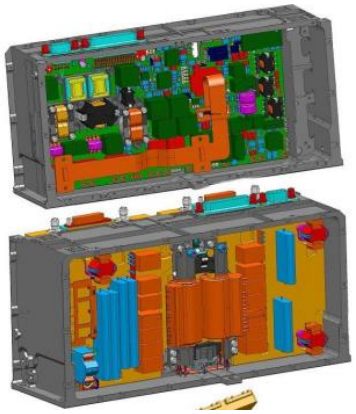

Overview: TWT Applications

Application fields for different types of TWT delay lines:

Application	**Communication**		**Radar and ECM**				
Sub-application	Ground Station	Space	Earth Observation	Ground & Ship Radars	Airborne Radars	Missile Seekers	ECM
Helix	x	x	x	x	x	x	x
Ring & Bar	x		x				
Coupled Cavity	x			x	x		
Interdigital Line	x			x	x	x	

TWTs for Ground Station, Airborne and Shipboard Communication

Depending on the system architecture, the microwave tubes used in ground-based, airborne or shipboard communication system transmit signals:

- to a satellite (up-link) or
- to a ground based receiver (point to point or point to multipoint communication).

Though in some communication systems, due to power requirements, also klystrons are used, TWTs are becoming predominant, because the relative bandwidth requirements are becoming more and more demanding (usually more than 10 % are required).

Survey on TED up-link TWTs for communication systems**:**

Frequency Band GHz	**C** 5.85 – 7.1	**X** 7.9 – 8.4	**Ku** 12.75 – 14.5	**Ku** 17.3 – 18.4	**Ka** 25.5 – 31.5	**Q** 43.5 – 45.5
Relative Bandwidth	up to 20%	6%	up to 13%	6.2%	up to 20%	4.5%
CW Output Power	3 kW	2.5 kW	1 kW	500 W	350 W	250 W

Some examples of ground-based or airborne communications systems using TED microwave tubes which are for commercial systems: DirecTV, Echostar and Astra for DBS, Iridium others are for military systems: Milstar, Syracuse, Stentor, SBIRS.

TWTs for Space Communication (I)

The major requirements for microwave tubes used in satellite transponders for transmitting down-link signals are:

- Long useful operating life and high reliability (>15years, <100 FIT (Failures In Time), respectively; more than 35,000,000 h accumulated in orbit)
- High total electrical efficiency (> 60%)
- High linearity (nonlinear phase shift < 48°)
- Low mass (depending on output power and radiation or conduction cooling)

TWTs meet all these demanding requirements and beat by far the competition from solid state amplifiers especially with respect to life, reliability and efficiency.

The driving force for the impressive improvements in all those parameters was in the past and is still today the economical pressure to save power by improving the efficiency and to reduce the mass of space amplifiers.

Two figures are best characterizing this environment:
The savings in launch and system costs per satellite are for

DC power saving 3,000 € / W and for mass reduction 20,000 €/kg.

TWTs for Space Communication (II)

Comparison of historic C-band tubes:

	First TWT in use	First Space TWT	First European Space TWT	Modern Space TWT
Program	TV-Ground link	Telstar 1	Symphonie	Measat
Manufacturer	STC	Bell Labs	AEG	TED
Year	1952	1962	1973	2003
Frequency	3.6 – 4.4 GHz	3.7 – 4.2 GHz	3.7 – 4.2 GHz	3.4 – 4.2 GHz
Output Power	2 W	2 W	13 W	70 W
Gain	25 dB	40 dB	46 dB	56 dB
Efficiency	1%	<10%	34%	71%
Nonlinear Phase	?	50°	50°	38°
Mass	>5,000g	>1,000g	640g	800g
Collector	1 stage	1 stage	1 stage depressed	4 stage depressed
Focusing System	Solenoid	PPM PtCo	PPM PtCo	PPM SmCo
Cathode	Oxide	Oxide	Oxide	MM Dispenser

TWTs for Space Communication (III)

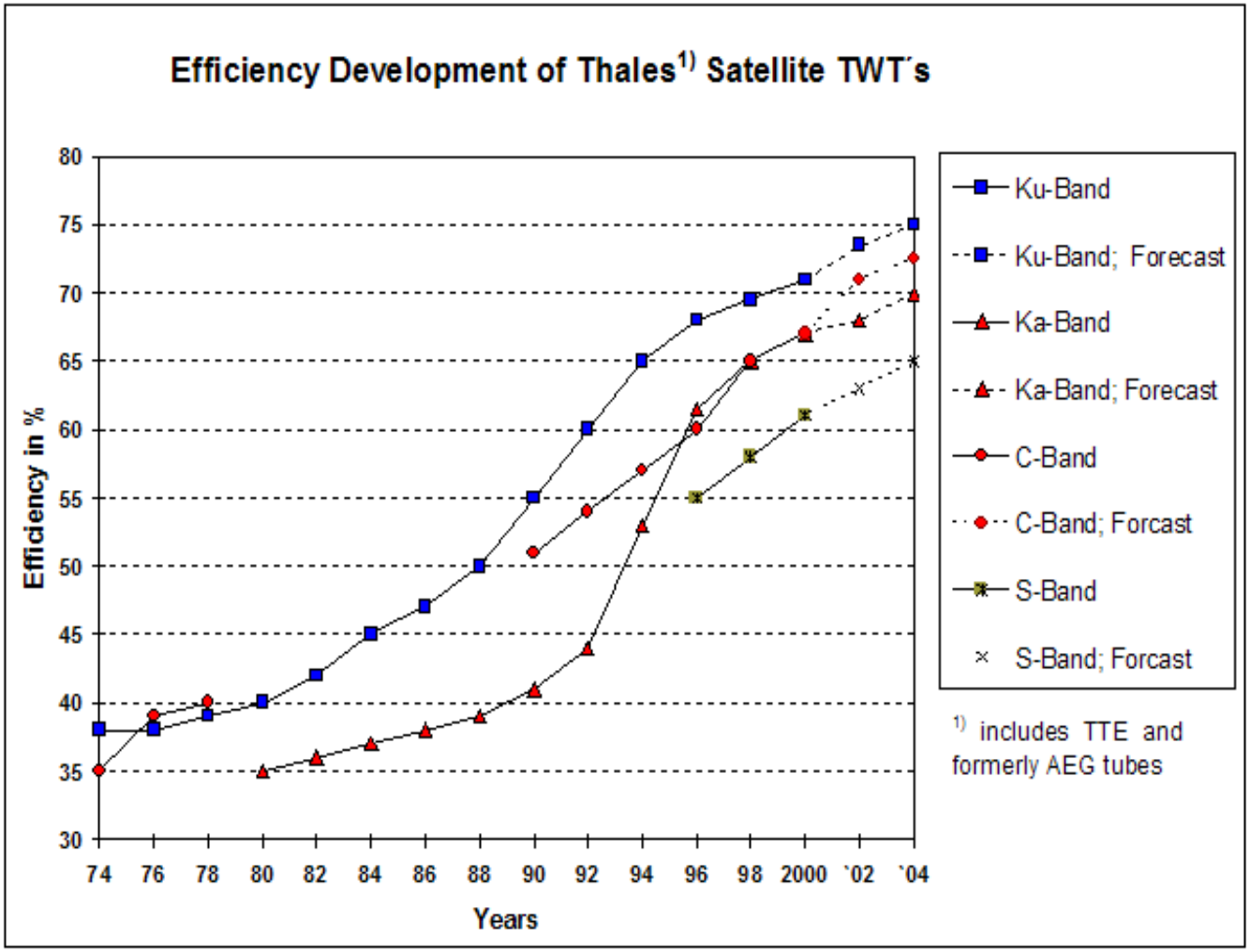

Efficiency improvement of space TWTs (courtesy of TED).

TWTs for Space Communication (IV)

Space TWT applications for communication and Earth observation:

Applications	Band Frequency / GHz	Power Efficiency	Future Trend Power Efficiency
Direct Digital Radio Navigation / GPS & Galileo	L-Band 1.1 – 1.5	50 to 150 W 55%	250 W 65%
Communication / TV-broadcast	S-Band 2.3 – 2.6	70 – 90 W 59%	120 W 65%
Direct digital radio for automotive	S-Band 2.3 – 2.6	200 – 240 W 61%	200 – 250 W 68%
Telecommuniation and broadcasting	C-Band 3.4 – 4.2	20 – 130 W 60 – 69%	150 W >73%
SAR for Earth observation, Radar TWT, pulsed	C-Band 5 – 6	5 kW 40%	>5 kW 45%
Scientific applications & deep space missions	X-Band 7 – 8.5	25 / 120 – 170 W 60%	25 / 120 – 170 W 65%
Earth observation, Radar TWT, pulsed	X-Band 7 – 8	4 kW 40%	>4 kW 45%
Telecommunication and broadcasting Internet Multimedia Services	Ku-Band 10.7 – 12.75	25 – 200 W 62 – 68%	25 – 300 W 68 – 75%
Altimeter; radar application for Earth observation, pulsed	Ku-Band 13 – 15 or 12 - 18	up to 100 W 55%	150 W 60%
Telecommunication and multimedia services	Ka-Band 17 – 22	15 – 130 W 55 – 66%	15 – 220 W 55 – 70%
Deep Space & Scientific Mission	Ka-Band 27 – 32	20 – 30 W 54 %	20 – 100 W 58%
Multimedia Services for low orbit satellites or stratosphere balloons	Q-Band 40 – 45	40 W 40%	40 – 100 W 40 – 45%
Inter-satellite links for multimedia services	V-Band 58 – 64	20 W 35%	20 – 100 W 35 – 40%

Radar and Electronic Counter Measurements (ECM) Klystrons and TWTs

Several types of microwave tubes for Radars: Magnetrons, Crossed-Field Amplifiers (CFAs), Klystrons and TWTs.

From a historical point of view, the magnetrons were the first microwave tubes to be used in radar transmitters, more than sixty years ago. But they are oscillators, and most of the radars, since several tens of years, require transmitters using a coherent amplification chain. Among the three types of amplifiers (CFAs, klystrons and TWTs), the TWTs are the most widely used, thanks to their wide instantaneous bandwidth, high gain and noise free coherent operation.

Surface Radars

Surface radars are ground based or are used in naval systems (shipboard radars). The main types of surface radars are:
- Long range surveillance radars for Air Traffic Control (ATC)
- Air defence radars
- Tracking radars
- Fire control radars: those are most time integrated into weapon systems
- Trajectography radars.

The table presents the relative bandwidth and the output power capability, as a function of frequency, for the TWTs (Ku and Ka band) and klystrons (up to and including X-band) made by TED for Surface Radars:

Frequency band GHz	L 1.25-1.35	S 2.7-3.5	C 5.4-5.9	X 8.5-10.5	Ku 15-18	Ka 33-36
Relative bandwidth	3%	3 to 15%	5 to 10%	10%	10 to 20 %	3 to 10%
Peak output power	4 MW	20 MW	1 MW	120 kW	2.5 kW	1 kW
Average output power	12 kW	20 kW	20 kW	5 kW	200 W	200 W

Airborne Radars

Microwave tubes (magnetrons and TWTs) are used in airborne radar transmitters in two categories:
- Multimode and multifunction radars: TWTs are widely used, either with CC slow wave structure or Helix.
- Terrain following radars: generally, TWTs are used.

Missile Seekers (Magnetron and TWTs)

The requirements for microwave tubes (magnetrons, klystrons and TWTs) used in active RF missile seekers are small size and weight, high electrical efficiency, very short start-up time, capability to withstand very severe environmental conditions and high reliability after long storage periods.

Some examples are: New generation MICA, ASTER and PAC3 missile seekers.

The main performances are presented in the table. It shows the relative bandwidth and the output power capability for magnetrons and TWTs made by TED for airborne radars or missile seeker applications, as a function of frequency.

Survey on missile radars:

Frequency band	X	X	X	Ku	Ka	W*
Type of tube	Helix TWT	CC TWT	Magnetron	TWT	TWT	TWT
Relative bandwidth (%)	20	3	Tunable in 600 MHz	20	3	1
Peak output power (kW)	20	120	220	2	1	0.15
Average output power (W)	800	1500	200	400	200	15

The Ka- and W-Band TWTs use interdigital delay lines; W* under development.

Broadband ECM Application TWTs (Electronic Counter Measurements: ECM))

The requirements for microwave tubes used in ECM systems are very wide instantaneous frequency bandwidth (more than one octave), small size and low weight and high electrical efficiency.

The only microwave tube which can meet a specification with more than one octave bandwidth is the Helix TWT. The table presents TED's helix TWTs made for ECM systems:

Survey on broadband ECM tubes against missile radars:

	Frequency band	6 to 18 GHz	18 to 40 GHz
Pulsed TWTs	Peak output power	2 kW	-
	Average output power	80 W	-
CW TWTs	CW output power	200 W	80 W

TWTs with High Average Output Power

Company	Frequency (GHz)	Power (kW)	Bandwidth (%)	Gain (dB)	
MLI	6	2.5	70	35	„Brazed Helix“
TED	6.5	3.0	20	48	„Brazed Helix“
Hughes	8	2.8	7	55	„Brazed Helix“
TED	8.2	2.5	6	52	„Brazed Helix“
TED	12.5	0.5	80	45	„Helix“
CPI	10	50	10	50	„Coupled Cavity“
CPI	16.7	26	12	46	„Coupled Cavity“
CPI	35	10	6	43	„Coupled Cavity“
CPI	94	0.8	1	40	„Coupled Cavity“